Corrosion Science 51 (2009) 1207–1227

Contents lists available at ScienceDirect

Corrosion Science

journal homepage: www.elsevier.com/locate/corsci

Review

A review of steel corrosion by liquid lead and lead–bismuth

Jinsuo Zhang *

Decision and Application Division, Los Alamos National Laboratory, Los Alamos, NM 87544, USA

ARTICLE INFO

Article history:
Received 2 February 2009
Accepted 5 March 2009
Available online 19 March 2009

Keyword:
Liquid metal,
Corrosion model
Corrosion inhibitor
C. Oxidation

ABSTRACT

Liquid metal technologies for liquid lead and lead–bismuth alloy are under wide investigation and development for advanced nuclear energy systems and waste transmutation systems. Material corrosion is one of the main issues studied a lot recently in the development of the liquid metal technology. This study reviews steel corrosion by liquid lead and lead–bismuth, including the corrosion inhibitors and the formation of the protective oxide layer. The available experimental data are analyzed by using a corrosion model in which the oxidation and scale removal are coupled. Based on the model, long-term behaviour of steels in liquid lead and lead–bismuth is predictable. This report provides information for the selection of structural materials for typical nuclear reactor coolant systems when selecting liquid lead or lead–bismuth as heat transfer media.

1. Introduction

One of the key limitations of design and application of liquid metal/alloy coolant systems in advanced nuclear reactors is the ability of available structural materials to resist corrosion. Liquid metal corrosion has been recognized to be one of the serious problems in use of liquid metal/alloy at high temperature systems and has been studied widely since liquid metals/alloys were considered to be candidates of the coolant of nuclear fast reactors. Compared with corrosion by aqueous media which has been found to be primarily an electro-chemical process, corrosion by liquid metal such as liquid lead and lead–bismuth alloy is a physical or physical–chemical process involving dissolution of material constituents, transportation in the two phases (liquid and solid) and reactions between corrosion products and impurities [1]. It has been reported that the corrosion by liquid metals/alloys can change the microstructure, composition, and surface morphology of the structural materials, which affects the mechanical and physical properties of the structural materials, etc., leading to a system failure. Therefore, liquid metal corrosion has been recognized as a failure of structural materials for advanced nuclear reactor systems as results of their high temperature physical and chemical interactions with liquid metals/alloys and containments.

Liquid lead or lead–bismuth eutectic (LBE) has been a primary candidate material for coolant in accelerator driven systems and in advanced nuclear reactors due to its favorable thermal–physical and chemical properties. However, corrosion of structural materials presents a critical challenge in the use of liquid lead and LBE in advanced nuclear reactors. Full knowledge of the important characteristics of the flow-induced and/or enhanced corrosion is essential in the proper design and safe operation of liquid lead/LBE heat transfer circuits.

Liquid lead and LBE corrosion is of great scientific and technological importance in the development of advanced nuclear reactors. It has developed into one of the important technologies in the field of nuclear science and engineering. During the last decade, a vast of literatures has been published as reviewed in two recent review publications [2,3]. In the present studies, we focus on review of the experimental data on corrosion and corrosion inhibitor and optimization of the protective oxide layer in liquid lead and LBE. The oxide layer growth data are analyzed by a corrosion model in which the oxidation and corrosion are coupled. The compositions of steels considered in the present studies are given in Appendix. Based on the present review and analysis, it is necessary to point out that the available experimental data are still very scattered and insufficient to develop corrosion/oxidation correlations between oxidation/corrosion rates and factors such as steel composition that affect the steel compatibility with liquid lead and lead–bismuth for nuclear power applications.

2. Corrosion and corrosion inhibitor

One of the effective methods for reducing the corrosion rate of structural materials by liquid lead and LBE is adding corrosion inhibitor to the liquid up to a certain concentration. By definition, a corrosion inhibitor is a chemical substance that when added in small concentration to an environment, effectively

* Address: International and Nuclear System Engineering, MS K-575, Los Alamos National Laboratory, Los Alamos, NM 87545, USA. Tel.: +1 505 667 7444; fax: +1 505 665 2897.
E-mail address: jszhang@lanl.gov.

0010-938X/$ - see front matter © 2009 Elsevier Ltd. All rights reserved.
doi:10.1016/j.corsci.2009.03.013

decreases the corrosion rate by forming a protective films which give the surface a certain level of protection. For liquid lead and its alloy LBE, the corrosion inhibitor can be roughly classified into two categories: metallic inhibitors and non-metallic inhibitors.

Most of the studies prior to 1980s for reducing the corrosion by liquid lead and LBE focused on the metallic inhibitors. The two general effective metallic inhibitors are Zr and Ti. Recently, oxygen was recognized to be an effective non-metallic inhibitor for liquid lead and LBE corrosion. The recent studies focus on how to control the oxygen level and what the protective oxide layer behaviour was in liquid lead and LBE environments.

2.1. Corrosion by liquid lead

The relative resistance to corrosion by liquid lead of 24 various metals and alloys were tested in a thermal convection loop with a temperature of 800 °C at the hottest section and of 500 °C at the coldest section [4,5]. The flow rate was estimated to be 0.5 cm/s. The mass transfer materials were collected in the bend at the bottom of the cold leg. Based on the test results, the test metals/alloys were divided into three groups [4]:

1. High corrosion resistance group included niobium and molybdenum. Neither of these metals suffered noticeable corrosion and mass transfer (deposition) under the test condition. It was reported there was no mass transfer for this group.
2. Mediate corrosion resistance group included Hastelloy B (67Ni–28Mo–5Fe), 410 and 446 stainless steel, Fe–14Cr–2Si, Ni–25Mo, Co–45Cr, Fe–50Mo, Fe–37Cr–16Ni, and Fe–50Cr. For this group, there was usually little mass transfer.
3. Low corrosion resistance group included Ni, Ta, Co, Cr, Fe, Be, Inconel, 304 and 310 stainless steels. For this group, there was heavy mass transfer, and the metals in this group also suffered relatively severe intergranular attack.

Therefore, of the 24 types of metals and alloys, only Mo and Nb were found to possess a high degree of resistance to mass transfer. The common structural and alloying metals such as iron, chromium and nickel were very inferior in this respect. Certain alloys of these metals, however, exhibited a considerable higher resistance to mass transfer, which could be attributed to intermetallic compound formation in the alloys [4].

Ni–Cr–Fe alloy, Nb, Mo, 304-, 347-, 446-stinless steels, and Armco Iron were tested in a loop with maximal temperature of 1073 K and minimal temperature of 773 K built in Oak Ridge National Laboratory (ORNL) [6]. The experimental results indicated that alloys with high Ni content (such as Ni–Cr–Fe alloy and 347 stainless steel) showed lower resistance to the corrosion by liquid lead compared with no Ni alloys. Similar to the result by Cathcart and Manly [4], Nb and Mo shows no corrosion. In another loop by ORNL, it was found that Croloy 2-1/4 (Fe–2.25Cr–1Mo) exhibited 25.4–203 μm of attack at 866–927 K, and Nb–1Zr showed no attack after 5280 h to lead at 1033 K [7].

Ali-Khan [8] reported that the corrosion rate of Cr and austenitic steel was in the range of 42–320 μm at 873 K for 1000- to 2000-h exposure, while Nb, Nb–5V, and V showed no attack at 898 K for 1858-h exposure. In these tests, it was also found that the corrosion rate increases with external stress in the materials, for example, the corrosion at the bend region of U shape sample was much higher than in the rest of other specimens.

In the two thermal loops [9] with a maximal temperature 823 K and a minimal temperature 470 °C made of Chromesco 3 steel and EM12 steel, the corrosion at the hot section was about 90 μm per 3000 h for Chromesco 3 and 30 μm for EM12. In the cold section, an abundant deposit of iron crystals up to several millimeters thick was formed on Chromesco 3 steel, while the deposition is much thinner (0–35 μm) on EM12. The lower corrosion rate of EM12 compared with that of Chromesco 3 steel was attributed to the fact that some protective oxide layer was found on the surface of EM12. Other tests by Asher et al. [10] in loops with maximal temperature 973 K and minimal temperature 823 K showed that Hastelloy N (68Ni–28Mo–5Fe) was severely attacked in only 4 days, and Croloy 2-1/4 was severely attacked in 15 days, and molybdenum showed no attack in 282 days.

James and Trotman's [11] results (Table 1) from a thermal convection loop with maximal temperature 1073 K and temperature difference 100 K show that the low-alloy steel has the highest resistance among the steel considered.

2.2. Corrosion by liquid bismuth

Liquid bismuth is more corrosive than liquid lead. Without adding inhibitor, the corrosion rate of the same materials by liquid bismuth is about 40 times greater than that by liquid lead at the same operation condition as shown in Table 1. Tests by James and Trotman [11] indicated that the steels containing large amounts of nickel and manganese had very low corrosion resistance in liquid bismuth due to the high solubility of these elements. Experimental results for the corrosion rate of different steels are given in Table 2, which confirmed the conclusion. A general trend of the corrosion

Table 1
Relative corrosion (mg/cm^2/h) of steels in flowing bismuth and lead. Temperature 1073 K and temperature difference 100 K [11].

Steel	Bismuth		Lead	
	No inhibitor	With 500 ppm Zr	No inhibitor	With 500 ppm Ti
0.3% C steel	1	0.01	0.032	0.001
Mild steel	1	0.01	0.034	0.001
CRM6	1.3	0.25	0.030	0.001
13% Cr–Fe	1.5	0.42	0.036	0.003
18Cr–8Ni SS	2.0	0.42	0.038	0.017

Table 2
Corrosion rates (mg/cm^2/h) for different steels in liquid bismuth [11].

Steel	Bi with Mg added at 700 °C with $\Delta T = 50$ °C	Bi with Mg and Zr added at 700 °C with $\Delta T = 50$ °C	Bi with Mg and Zr added at 800 °C with $\Delta T = 80$ °C
89348	1.10	<0.006	0.857
G.7682	1.33	<0.006	1.34
57818	1.41	<0.006	1.61
Mo–Cr	1.23	<0.006	1.67
19477	1.42	<0.006	1.79
CRM6 (nitrided)	1.46	<0.006	1.96
86217	1.46	<0.006	2.18
Mo–V	1.46	<0.006	2.38
Mild steel	1.21	<0.006	2.38
23021	1.46	<0.006	2.38
CRMO	1.52	<0.006	3.04
CRM6 (G.7524)	1.48	0.018	–
CRM6 (G.7824)	1.65	0.190	–
Chrom Va–W	1.39	0.387	–
008853	1.53	0.387	–
1.89% Si–Fe	1.05	0.327	–
12% Cr–Fe	1.77	0.518	–
18-8 SS	2.48	0.518	–
Fe	1.27	1.161	–

rate was made as [11]: 18-8 Stainless steel > 13% Cr–Fe > low-alloy steels, which indicates that the corrosion rate increases with Cr content increasing. However, this trend can only be applied to the cases of clear bismuth or oxygen getter such as Mg is added. If there is oxygen in the liquid, the oxide layer forming on the surface can protect the materials, resulting in an inverse trend: the corrosion rate decreases with the content Cr increasing in steels, which was reported by Wilson et al. [12] and noted by James and Trotman [11].

The effects of the content of Ni and Mn in the steel on the corrosion rate by bismuth are equally deleterious [11]. Experimental result for CRM6 steels with different total content of Mn and Ni are shown in Fig. 1. Although the results are scattered, the trend is that the corrosion rate increases with content of Mn and Ni increasing as shown by the fitted line in the figure.

The corrosion rate of 2.25 Cr–1Mo steel in liquid bismuth was studied by Horsley and Maskrey in convection loops [13]. The results indicate that the corrosion rate is at least 16.51 mm/yr in the temperature range of 748–898 K with flow velocities of 3–4 mm/s. Test results by Deville and Foley [14] indicate that the corrosion rate of 2.25Cr–1Mo steel in flowing liquid bismuth is affected by the heat treatment applied on the specimen. Waide et al. [15] discussed an in-pile corrosion test loop made of 2.25Cr–1Mo steel operating at temperatures 773 K and 748 K.

Carbon steels with varying content of Cr were examined by Dawe et al. up to 823 K in liquid bismuth [16]. It was reported that a 12% Cr steel showed the least mass transfer rate, and no corrosion was observed after 2500 h of operation. In a loop made of 347 stainless steel [17], after 100-h operation with maximal temperature 900 °C and temperature difference 280 K, only limited corrosion was observed.

2.3. Corrosion by liquid lead–bismuth alloys

Along with the studies on corrosion by liquid lead and bismuth, studies on the corrosion by liquid lead–bismuth alloy were carried as early as 1950s. Cygan seems to be the first researcher who built two convection loops to study the corrosion of several steels in flowing lead–bismuth alloy [18,19]. One loop was made of low-carbon steel (1015 steel) and the other one was made of 400-series steels. The maximal temperature is 727 K and the temperature difference is about 273 K. The flow velocity was in the range of 3.3–8.8 cm/s. When a small pocket containing a permanent magnet was attached to the cold leg exit, the low-carbon steel loop was able to operate for over 11,000 h, without stopping by stoppage of the flow path. Experimental results were summarized by Park and Buksa [7]. as follows:

1. When a steel surface is not completely deoxidized, impurities (Bi_2O_3, Pb_3O_4) rather than corrosion products appeared to be the major factors resulting in the stoppage of passage;
2. a possible method of metal purification might be the use of magnetic trap;
3. low-carbon steel appeared to be a useful container for the liquid up to 727 K; and
4. there was no advantage in using 410 or 446 stainless steel up to 727 K.

Failure was reported in loops made of 347 and 430 stainless steel, which was because of the plugs formed by mass transfer products [20].

Romano et al. [21] measured the corrosion rate of Croloy 1-1/4 (Fe–0.15C–1.25Cr–0.5Mo) steel in liquid Pb–Bi solution by running loops at a temperature up 923 K and an average velocity of 1.5 cm/s. Results are summarized in Table 3. Clearly, without inhibitor added, Croloy 1-1/4 cannot be used as the container materials of liquid lead–bismuth alloys.

The corrosion rate of steel exposed to liquid lead–bismuth alloy depends on the liquid composition. The corrosion rate as a function of Pb and Bi content in the liquid alloy obtained by Ilincev [22] is shown in Fig. 2. Clearly, the corrosion rate of the same steel increases with increasing the content of Bi. The figure also shows that corrosion rate is almost linear to the activity of Bi. Based on this phenomenon, the author suggested a correlation to estimate to the corrosion rate (R_{Pb-Bi}) by liquid lead–bismuth alloy if the corrosion rate constants by liquid lead (R_{Pb}) and bismuth (R_{Bi}) were known:

$$R_{Pb-Bi} = R_{Bi}a_{Bi} + R_{Pb}a_{Pb}, \quad (1)$$

where a_{Pb} and a_{Bi} are the activity of Pb and Bi in the liquid metal alloy, respectively. The figure also shows that the corrosion rate increases with the content of Cr in the steel increasing, which is same to the cases in liquid bismuth and lead.

Fig. 3 shows corrosion rate of some steels in liquid Pb, Bi and Pb–Bi as a function of temperature [22]. As shown in the figure, liquid bismuth is the most corrosive among the three types of liquids. All the corrosion rate functions exhibit an exponential trend. Based on the figure, Ilincev [22] concluded that the steel corrosion was not dependent on the number of alloying elements; prolonged exposure and extraction of elements more prone to dissolution, such as Ni, Mn and Cr, left corrosion of various types of steel to be determined mainly by the dissolution rate of the primary element, i.e. Fe.

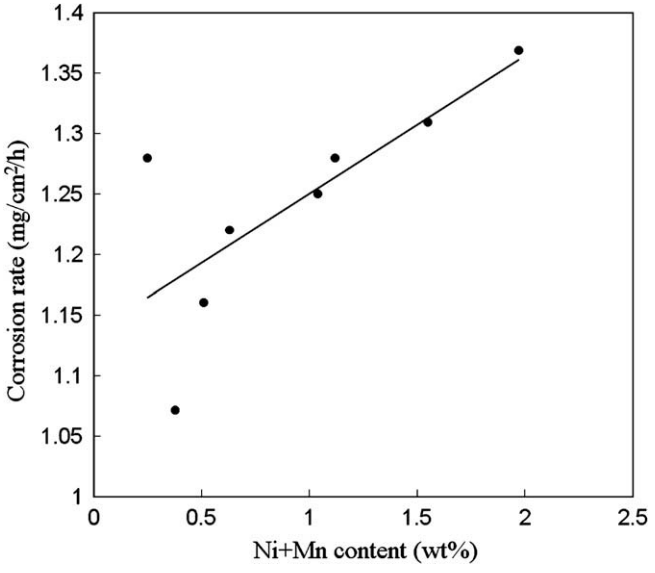

Fig. 1. Corrosion rate against the total content of Ni and Mn. Experimental results [11] from a loop with a maximal temperature of 823 K and $\Delta T = 100$ K.

Table 3
Corrosion of Croloy 1-1/4 steel in flowing LBE [21,7].

Temperature (°C)	Time (h)	Inhibitor	Results
500–625	<1000	No	Severe corrosion
400–550	1000–5000	No	Severe corrosion
625	<100	No	Severe corrosion
350–650	<5000	Ti added	No corrosion
200–400	<10,000	No	No corrosion
500–650	<10,000	Zr added	No corrosion

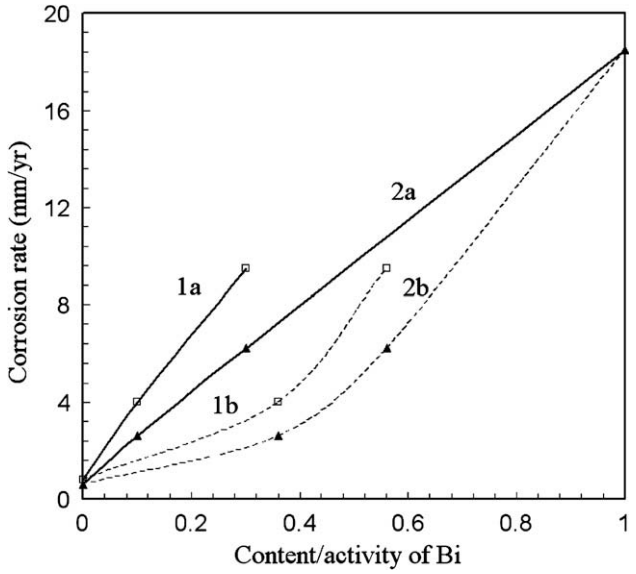

Fig. 2. Corrosion rate as a function of content (1b and 2b)/activity (1a and 2a) of Bi [22]. 1a and 1b: 18Cr–9Ni-type stainless steels; 2a and 2b: low-alloy highest-creep-strength steel 0.5–2.0% CrMoV. The results were from a loop with a maximal temperature of 873 K with a temperature difference 140–150 K and a flow velocity of 1.0–1.5 cm/s. Mg (500 ppm) was added to the liquid to get the oxygen.

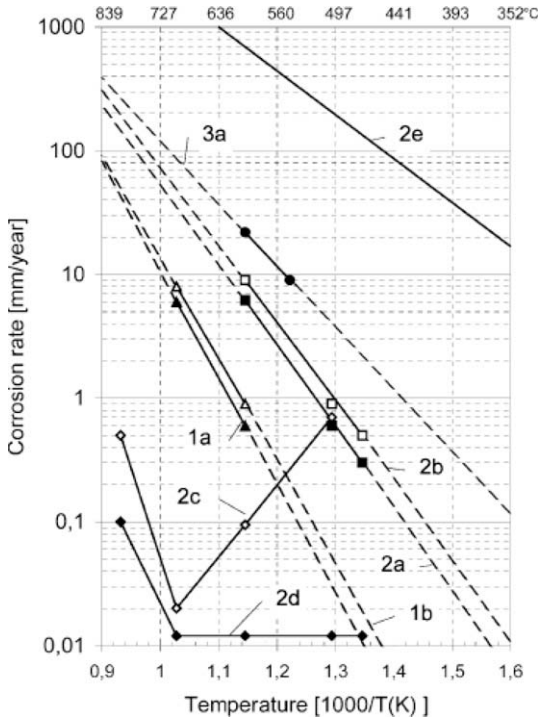

Fig. 3. Steel corrosion as a function of temperature in Pb (1), Pb–Bi (2) and Bi (3) deoxidized with 500 ppm Mg (a and b) or with 20–100 ppm Ti/Sr corrosion inhibitor and 500 ppm Mg (c and d) under a condition with a temperature difference of 150 K and flow velocity of 1.0–1.5 cm/s. 1a, 2a, 2d and 3a: carbon and low-alloy CrMoV (up to 2% Cr) steels; 1b and 2b: 18Cr–9Ni-type stainless steels; 2c: Steels containing 3–5% CrMoW/V; 2e: Corrosion of metal Ti in Pb–Bi [22].

2.4. Metallic inhibitors

Tables 1–3 as well as Fig. 3 show that the corrosion rate by liquid lead, bismuth and lead–bismuth can be significantly reduced through adding Zr or Ti into the liquid. Titanium and zirconium are typical corrosion inhibitors for the corrosion by liquid lead/bismuth. It has been reported that the addition of 50–500 ppm of zirconium or titanium to the liquid heavy metal can inhibit corrosion of steels by reacting with nitrogen and carbon from the steel to form inert, adherent surface layers of ZrN, TiN, or TiN + TiC [23] which were found to be entirely compatible with liquid Bi and Pb [24].

Considering that the protective film is formed by the chemical reaction between the inhibitor (Zr or Ti) in the liquid with the carbon as well as the nitrogen in the steel, the content of N and C in the steel plays important role on the inhibition efficiency. Corrosion of iron [11] with different content of N and C in liquid bismuth is shown in Table 4. The weight loss decreases with the total content of the N and C in iron. However, the carbon seems to be more efficient than nitrogen based on this table, which can be also drawn form results in Table 2. Different from these results, results by Horsley and Maskrey [13] indicate that the inhibition efficiency depends strongly on the nitrogen content in the steel, for steel 2.25Cr–1Mo in liquid bismuth, the corrosion rate reduced to 0.254 mm/yr from 16.51 mm/yr by increasing the nitrogen content to 1.0% and the experimental tests also showed that it was possible to reduce the corrosion rate to 0.0254 mm/yr. The nitrogen effects were also found in liquid lead [10].

For steel with high content of Cr such as 13Cr–Fe and 18Cr–8Ni stainless steel, the corrosion rate is still very high as shown in Tables 2 and 3, indicating that the inhibition efficiency depends on not only the content of C and N but also some other active consistent such as Cr, Si, W since these elements govern the availability of carbon and nitrogen at the liquid/solid interface. Ilincev [22] concluded that for low- and medium-alloy steels, adding Zr and Ti in the liquid could prevent corrosion almost completely at temperature below 973 K and partially even at 973–1073 K, but stainless chromium–nickel steels were not subject to inhibition.

Comparison of the microphotography of steels exposed to LBE without inhibitor and of a steel exposes to LBE with an inhibitor was shown in Fig. 4. Clearly, without inhibitor added, the corrosion attack by LBE was more than 40 μm as shown in Fig. 4a after 300-h exposure. However, with 10–40 ppm Ti added, no corrosion attack layer was observed even after 6000-h exposure in LBE as shown in Fig. 4b.

It was necessary to continue adding inhibitor during operation to main the protective layer [21]. Recently an experiment [25] showed that the previous TiN coating on steel surface is promising protection and the layer seems to be not influenced by neither LBE nor static stress up to 200 MPa after 6000-h exposure. However, this experiment was carried out at a low temperature 623 K, it is hard to conclude that we do not need to supply the inhibitor to main the inhibitor layer after it is formed at a higher temperature.

Without oxygen getter, tests were carried out in a loop with a Zr pipe incorporated [26]. Zr entered into LBE through spallation of the previous formed ZrO_2. It was found that Zr in LBE inhibited the corrosion and affected the interaction layer between LBE and steel, but this effect is not due to forming a protective layer but due to consumption of oxygen in LBE by the presence of Zr. At

Table 4
Weight loss of iron after two week exposure to inhibited bismuth at temperature 1023 K and temperature difference 50 °C [11].

Carbon (%)	Nitrogen (%)	C + N (%)	Weight loss (mg)
0.0041	0.0288	0.0698	170
0.085	0.0288	0.1138	30
0.234	0.0288	0.2628	<1
0.0041	0.0385	0.0426	141
0.0041	0.31	0.3141	33

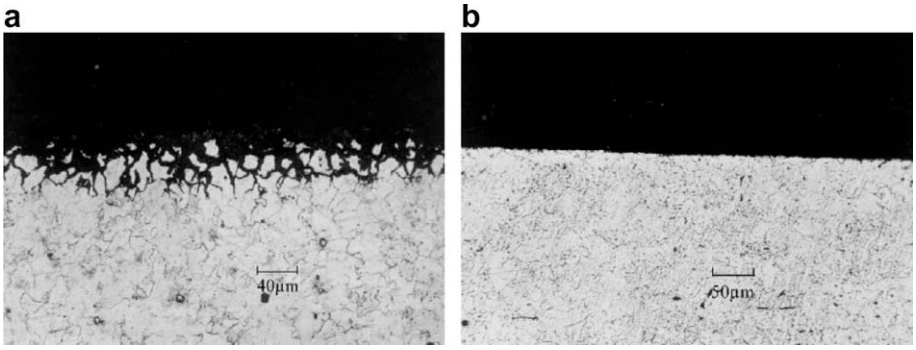

Fig. 4. Microphotography of (a) attack of 2CrSiMoV steel after 300 h in LBE without inhibitor and (b) protect of CrMoV steel after 6000 h in LBE with 10–40 ppm Ti. The experiments were carried out at 873 K with 300–500 Mg added for oxygen getter [22].

higher temperature, a layer of Zr compounds (oxides and nitrides) was observed on the steel surface. However, the layer was found not to be tightly adhered and it was liable to spall off.

Metallic inhibitor such as Ti and Zr in liquid lead and LBE inhibits the corrosion by reactions on the steel surface with minor constituent of the steel such as N and C. The reactions result in a surface layer such as (Ti, Zr)N or (Ti, Zr)C, which severe as a barrier to prevent dissolution of the steel components into the liquid lead or LBE. Therefore, any factor that affects the N and C activity in the steel will affect the inhibition efficiency.

The possible stable nitrides [27] in steels are ZrN, TiN, AlN, TaN, VN, Si_3N_4, Mn_xN_y, Cr_2N, Mo_2N. Considering that Zr, Ta and Ti are not commonly presented in steels, then increasing any of the left elements (Al, V, Si, Mn, Mo, Cr) will reduce the N activity in the steel and affect the formation of the protective inhibitive layer.

It was reported that there was a critical C concentration below which the inhibition efficiency is low [27]. The critical concentration is significantly close to the value required to form $Cr_{23}C_6$, indicating that the excess carbon above the critical concentration is beneficial to the inhibition film formation.

Through comparing the experimental results and theoretical prediction, Weeks and Klamut [27] concluded that the formation of nitride film was controlled by the nitrogen diffusion through the film, while the carbide film was controlled by the carbon diffusion in the steel. Comparison between zirconium and titanium indicates that zirconium appears to be the most effective inhibitor. The required concentration of zirconium in the liquid is slightly easier to maintain than titanium, also zirconium has a lower thermal neutron cross-section than titanium [7].

2.5. Summary on corrosion by liquid lead, bismuth and LBE and metallic inhibitor effects

1. There is no significant difference between the corrosion mechanisms of liquid lead, LBE and bismuth. Among the three liquids, bismuth is the most corrosive, while LBE is in the middle. For liquid lead–bismuth alloys, the corrosion rate increases almost linearly with activity of bismuth in the liquid alloy.
2. Without corrosion inhibitor added, Mo has a high corrosion resistance to the liquid metal and can be used as the contained materials. The corrosion of carbon steels, low-alloy steels and stainless steels is severe, and all these materials cannot be used as the container materials for liquid lead, bismuth, and LBE.
3. Zr and Ti are effective metallic inhibitors for carbon steels and low-alloy steels, while for stainless steels the inhibition efficiency is low.
4. The inhibition mechanism is to form a thin protective film through reactions between the inhibitor (Zr, Ti) and the minor constituents of the steel (nitrogen and carbon). The film is composed of (Zr, Ti)N or (Zr,Ti)C, or compounds.
5. The formation of nitrides is controlled by the diffusion of nitrogen through the film, while the formation of carbides is controlled by the carbon diffusion in the steel.
6. The affinity of Ti and Zr to form nitrides is higher (2–3 times [22]) than carbon. Therefore, if enough active nitrogen is presented in the steel, protective nitride film will form, and after consuming of all active nitrogen, carbide film will start to grow.
7. The inhibition efficiency is a function of the composition of the steel. Any factor that reduces the activity of the nitrogen and carbon in the steel will reduce the inhibition efficiency.
8. The film adheres to the steel surface, while film spalling can occur. Subsequently new film can form in the corroded region [27].
9. Oxygen getter such as Mg needs to be added; otherwise the film composed of nitrides and oxides does not tightly adhere.

2.6. Non-metallic inhibitor effects

Oxygen has been found to be an effective non-metallic inhibitor in liquid lead and LBE systems. Instead of reaction with minor constituents of the steel like the metallic inhibitors, the oxygen reacts with the major components of the steel such as Fe, Cr and Ni to form a protective oxide layer.

The active oxygen control technique [28] exploits the fact that lead and bismuth are chemically less active than the major components of steels, such as *Fe, Ni,* and *Cr*. By carefully controlling the oxygen concentration in LBE, it is possible to maintain an iron and chromium based oxide film on the structural surfaces, while keeping lead and bismuth from excessive oxidization that can lead to precipitation contamination. The oxide film effectively separates the substrates from the liquid metal. Once this oxide film is formed on the structure surface, the direct dissolution of the structural materials becomes negligible because the diffusion rates of the alloying components are very small in the oxides layer.

For example, an experimental result [29] on the effects of oxygen in liquid lead on the corrosion behaviour of steels is shown in Fig. 5. For oxygen concentration below 10^{-7} at.% in lead, corrosion is determined by dissolution of alloy components because no effective oxide layer was formed and the corrosion rate increases significantly with decreasing oxygen concentration. Otherwise, if the oxygen concentration is greater than the value of 10^{-6} at.%, oxide films forms on steel surfaces that can prevent the direct dissolution of alloy components. The oxide film thickness depends strongly on the oxygen concentration, and with oxygen concentration increas-

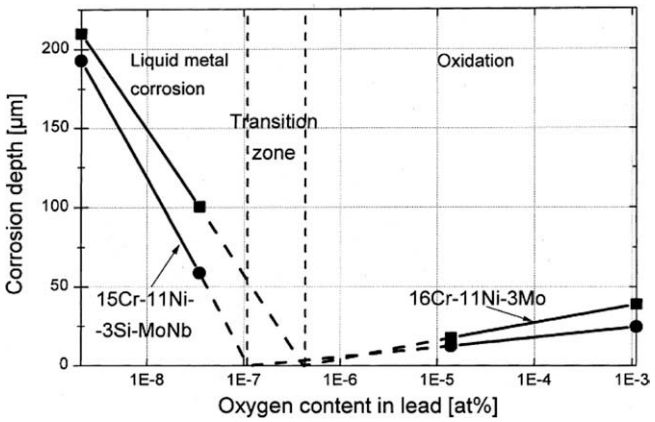

Fig. 5. Oxygen concentration effects on corrosion behaviour of steels in flowing liquid lead after 3000 h at 550 °C [29].

ing, heavy oxidation results in deep corrosion attack as shown in the figure. Therefore, to avoid heavy dissolution and oxidation as well as to remain/restore the protective oxide films, the oxygen concentration in lead alloys needs to be actively controlled.

It should be noted that the inhibition efficiency of oxygen depends not only on the oxygen concentration in the liquid, but also explicitly on steel/oxide compositions/microstructures. From the materials perspective, higher concentrations of alloying elements that can form stable, adherent and dense oxides should reduce the oxidation/corrosion rate. Consequently, for ferritic/martensitic steels, higher concentrations of Cr, Si, or Al result in lower oxidation rate and thinner protective oxide layers.

It has been found that oxygen control in liquid lead and lead–bismuth for applications of nuclear power systems is an effective method to reduce the corrosion and enhance the structure life time. An ideal protective layer should be pore-free, crack-free and stress-free at operating temperatures. For practical lead-alloy systems, it is nearly impossible to attain such an ideal protective layer throughout the varying environment. However, it is possible to achieve acceptable performance by controlling oxygen level in liquid metals, adjusting steel compositions or surface conditions, system configurations or operating conditions. Recently studies focus on characterizing the properties of the oxide layer forming under liquid lead and LBE environments and finding techniques to enhance the protective efficiency.

3. Oxidation of steels in liquid lead under oxygen controlled

The main components of common steels such as Fe, Cr and Ni have lower solubility in liquid lead than in LBE in a considered temperature range [2,3], resulting in lower corrosion rate in liquid lead. However, liquid lead is still a corrosive media, and without protection the corrosion of steels by liquid lead for the application of nuclear coolant is not acceptable. Oxygen control technology has been developed o form protective oxide layers to increase the corrosion resistance of the steel exposed to liquid lead. In this section, we will review the experimental data on the oxidation of steel in liquid lead under controlled oxygen concentrations.

3.1. Oxidation of steels in static liquid lead

The easy way to study the oxidation of steel in liquid lead with oxygen control is to insert a sample into liquid lead in a static capsule whose temperature is easily to be controlled. However, it is necessary to notice that the results from an experiment of a static capsule cannot be applied directly to a flow system because the effect of flow velocity is not included.

3.1.1. AISI 316L steel

Samples of AISI 316L steel were tested at temperature 737 K in static liquid lead with saturated oxygen for 700 and 1200 h [30]. It was found that the oxide layer was very thin and the thickness was in the range of 2–4 μm after 1200-h exposure. Ni was accumulated at the interface between the oxide layer and the steel. The composition of the oxide layer is $Fe(Fe_{1-x}Cr_x)_2O_4$. The oxide layer was protective.

3.1.2. 1.4790 steels

Austenitic steel 1.4790 was tested at 823 K in liquid lead with an oxygen concentration 0.06 ppm up to 300 h [31]. Duplex oxide layer structure was found as well as an oxygen diffusion layer underneath the oxide layer. The outer layer of the duplex oxide layer was composed by Fe_3O_4, while the inner layer was composed by $Fe^{2+}(Fe^{3+}_{1-x}Cr^{3+}_x)_2O_4$, containing Pb. It was found Ni was strongly depleted in the inner oxide layer, while it was accumulated at oxide/steel interface. The thickness of the oxide layer could research 16 μm after 3000-h exposure.

If the surface of the sample was treated by pulsed electron beam (GESA) which leads to finer grain at the surface area, the thickness of the outer layer and the oxygen diffusion layer could be reduced significantly. If the surface was treated by Al-alloyed, no oxide layer and depletion of Ni was found. The thickness of the outer, the inner oxide layer and the oxygen diffusion layer of 1.4790 steel is given in Table 5.

3.1.3. Mod. F82H steel

Samples of F82H steel were tested at 793 K in static liquid lead with oxygen saturated for 2000 and 3700 h [32]. The average thickness of the oxide layer was about 20 and 40 μm after exposed for 2000 and 3700 h, respectively. The weight of the sample was increased. The oxide layer has a double-layer structure as shown in Fig. 6 [32].

The outer layer, composed by Fe_3O_4 was not compact and has columnner morphology. Metallic lead was detected in the outer layer, while no Fe–Pb–O ternary compound was found. Compared with the outer layer, the inner layer was more compact and was composed by $(FeCr)_3O_4$. The thickness of the two sublayers increases along with the exposure time, indicating that the layer itself is not protective against oxidation in oxygen-saturated liquid

Table 5
Materials and test data after exposed to static liquid lead with an oxygen concentration of 0.06 ppm at 823 K [31].

Steel	Treatment	Time (h)	Inner layer (μm)	Outer layer (μm)	Diffusion layer (μm)
OPTFER	Original	3000	20	15	10
	GESA	3000	16	15	8
	Al-alloyed	1500	None	None	None
1.4970	Original	3000	10	6	12
	GESA	3000	6	6	3
	Al-alloyed	1500	None	None	None

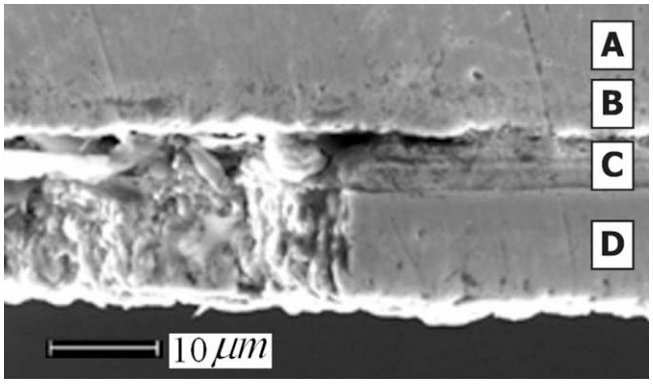

Fig. 6. Cross section of a corrosion layer grew on uncoated F82H exposed to liquid lead at 793 K for 2000 h [32]. The left side of the layer shows a fracture section (A: steel; B: Cr-depleted steel; C: Me_3O_4 with Me.Fe, Cr; D: Fe_3O_4 embedding small particles of lead).

lead containing an additional source of oxygen. On the other hand, Cr-free sublayer might have favored the embedding of very small particles of metallic lead [32].

Duplex oxide structure was also reported at a lower temperature (737 K) at oxygen saturation for 700- and 1200-h exposure [30]. The outer layer was also found to be Fe_3O_4 with particles of metallic lead, while the inner layer was found to be spinel $Fe(Fe_{1-x}Cr_x)_2O_4$. The outer layer, having columnar morphology, was typically grown along the direction of the diffusion species.

At temperature 793 K and oxygen saturation, No significant weight change or alteration was observed on the aluminized samples after exposed for 3700 h [32]. No oxide layer was detected by XRD. However, it was possible to think that the oxide layer Al_2O_3 was formed on the surface which had a very thin thickness and was against the oxidation and corrosion. Then one can conclude that the aluminized coating can protect the steel from both oxidation and corrosion during the exposure to liquid lead at this temperature.

3.1.4. OPTIFER steel

Samples of OPTIFER steel were tested at 823 K in static liquid lead with 0.06 ppm oxygen [31]. Three kinds of attack layers were investigated at the surface area: a duplex oxide layer and a diffusion layer under the oxide layer. The outer oxide layer that ended at the original specimen surface, consisted of magnetite without appreciable Cr concentration. This layer was brittle because many

Table 6
Summary of the experimental results of steel tested in static liquid lead with oxygen control.

Steel	Temp. (K)	Oxygen (ppm)	Time (h)	Thickness (μm)	Composition
1.4790	823	0.06	800 1500 3000	2.5 4.0 12	Duplex structure, outer layer: Fe_3O_4, Inner layer: $Fe^{2+}(Fe_{1-x}{}^{3+}Cr_x{}^{3+})_2O_4$+Pb, oxygen diffusion zone
1.4790-GESA	823	0.06	800 1500 3000	3.0 5.0 6.0	Duplex structure, outer layer: Fe_3O_4, Inner layer: $Fe^{2+}(Fe_{1-x}{}^{3+}Cr_x{}^{3+})_2O_4$+Pb, oxygen diffusion zone
1.4790-alumized	823	0.06	800 1500 3000	None None None	
20Kh13	923	0.1–0.4	3000	Very thin	Intermediate layer: Same compositions as the steel+Pb, oxide layer: $FeCr_2O_4 + Cr_2O_3$ compounds
20Kh13	923	Sat.	50 100 200 500	12 17 25 30	Duplex structure, outer layer: $(Fe_{1-x}Pb_x)O{\cdot}Fe_2O_3$; inner layer:$(Fe_{1-x}Pb_x)O{\cdot}(Fe_{1-y}Cr_y)_2O_3$
AISI 316L	737	Sat	700 1200	None 2–4	$Fe(Fe_{1-x}Cr_x)_2O_4$
EP823	923	0.01–0.1	3500	<0.1	Duplex layer, outer layer: Fe–based oxide compounds; inner layer: Cr-based oxide.
Mod. F82H	793 737	Sat Sat	2000 3700 700 1200	~20 ~40 8 20	Duplex oxide layer, outer layer: Fe_3O_4 + Pb, inner layer $(FeCr)_3O_4$. Duplex oxide layer, outer layer: Fe_3O_4+Pb, inner layer $Fe(Fe_{1-x}Cr_x)_2O_4$
Mod. F82H aluminized	793	Sat	2000 3700	None None	
OPTIFER	823	0.06	800 1500 3000	12 17.5 30	Duplex structure, outer layer: Fe_3O_4, inner layer: Fe–Cr spinel, oxygen diffusion zone
OPTIFER GESA	823	0.06	800 1500 3000	11 17.5 31	Duplex structure, outer layer: Fe_3O_4, inner layer: Fe–Cr spinel, oxygen diffusion zone
OPTIFER Al-alloyed	823	0.06	800 1500 3000	None None None	
Fe–16Cr	923	Sat	17	30, then exfoliation	Outer lyer Fe3O4 + Cr2O3 particles + Pb
Fe–16Cr	923	0.48	1000	Not measure	Four different zones
Fe–16Cr–1Al	923	Sat	13	20 then exfoliation	Outer layer Fe3O4 + Cr2O3 particles + Pb
Fe–16Cr–1Al	923	0.48	1000	50–60	Four different zones

defects exited caused by spallation of scale parts. In the inner oxide layer, composed Fe–Cr spinel, rooted in the pore belt. At some place, the spinel layer was not found. The thickness for the different layers is given in Table 5.

If the surface was treated by an electron pulse (GESA) before the test, the size of the magnetite scale is smaller and more compact than that of the untreated surface. However, this layer could also spalled off. If the surface was treated by Al-alloyed, no oxidation and no corrosion were reported.

3.1.5. EP823 steel

Samples of EP823 steel were tested in stagnant oxygen-containing liquid lead in an oxygen concentration range of 0.01–0.2 ppm at 923 K up to 3500 h [33]. Before testing, the sample was subjected to a procedure of thermal treatment in vacuum, after which a very thin (~20 nm) Cr-based oxide layer was formed on the surface. After holding in the liquid lead for 20 h, the thickness of the oxide formed in the stage of thermal treatment became thicker and the silicon content in the oxide increased. It was found that the growth of the oxide layer occurred most intensely at the sites of appearance of grain boundary on the surface and propagated in the course of time over the entire surface. With increasing the test time up to 3500 h, the iron-based oxide layer was observed on the top of chrome-based oxide layer. No lead was found in the oxide. The oxide film formed on the surface of EP823 steel at such test condition was protective.

3.1.6. 20Kh13 steel

Such steel was tested at a temperature range of 873–973 K in stagnant liquid lead with oxygen concentration in a range of 0.1–0.4 ppm [34]. It was found that a heterogeneous structure was formed in the interaction zone. The structure consists of an external intermediate layer, a thin oxide film and porous substrate layer. The intermediate layer, having the same compositions as the steel, appeared very inhomogeneous at the interface. The density of this layer significantly decreases with decreasing the distance from the matrix. Lead was found to be accumulated at the boundaries. This layer has very poor adhesion to the surface and can be readily removed.

The oxide layer, separating the substrate from the intermediate layer, was found to be very thin and composed of $FeCr_2O_4$ and Cr_2O_3 compounds. The layer is too thin to be detected by X-rays. However, this film inhibited the process of penetration of lead into the matrix, but it could not prevent the process of diffusion of components of the matrix into the liquid. As a result, vacancies were found in the substrate in the interaction area. These vacancies were accumulated on the structural defects and formed a porous zone penetrable for oxygen in the surface area.

The 20Kh13 steel was also tested in stagnant liquid lead saturated with oxygen (~60 ppm) at 923 K up to 500 h [35]. Very different phenomena were found compared with the tests in liquid lead with lower oxygen concentration. Duplex oxide layer was formed on the steel surface. The outer layer was composed of $(Fe_{1-x}Pb_x)O{\cdot}Fe_2O_3$ and the inner layer was composed of $(Fe_{1-x}Pb_x)O{\cdot}(Fe_{1-y}Cr_y)_2O_3$. Both layers symmetrically grow with respect to initial "solid-melt" interface. Lead was not found in the substrate and it was fixed only in the oxide layer.

3.1.7. Fe–16Cr and Fe–16Cr–1Al alloys

Fe–16Cr and Fe–16Cr–1Al alloys were tested at 923 K in stagnant liquid lead with different oxygen concentrations [36,37]. For low oxygen concentration (<0.01 ppm), a very thin oxide layer (1–5 μm) formed on the surface which was composed of Fe_3O_4 after 1000 h. Lead was found in both the oxide layer and the substrate. The concentration of chromium at the surface under the oxide layer was substantially increased due to the outwards diffusion of iron. The oxide layer could not prevent the diffusion of iron and the penetration of liquid lead.

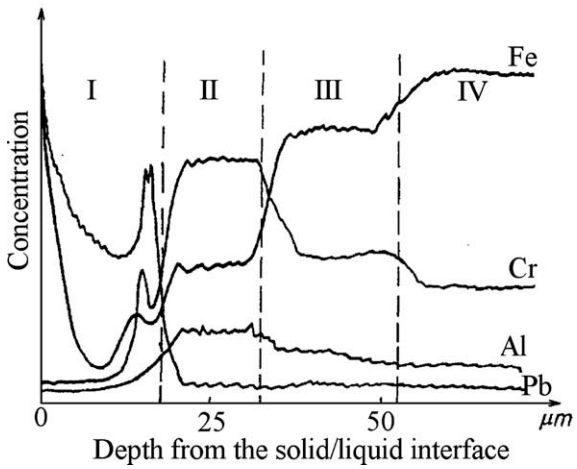

Fig. 7. Distributions of elements in oxide films on the surface of Fe–16Cr–1Al alloys tested for 1000 h in static liquid lead with 0.48 ppm oxygen [36].

As increased the oxygen concentration to saturation, the composition and the structure of the oxide layer were substantial changed. For example, the thickness of oxide layer formed on surface of Fe–16Cr–1Al alloys was about 50–60 μm after 1000 h and its structure had four different zones as shown in Fig. 7 based on the compositions of the layer. The Zone I was characterized by the presence of a porous surface oxide layer with high concentration of iron and lead and low concentrations of chromium and aluminum. The main composition of this layer was magnetite and lead. The Zone II was composed of a Fe_3O_4–$FeCr_2O_4$ solid solution with the structure of the spinel. Compared with the composition of Zone I, the concentration of chromium and aluminum was enriched in this layer. Zone III was formed by a solid solution based on α-Fe and enriched with chromium and aluminum. Internal oxidation was observed, which resulted in the formation of chromium and aluminum oxides mainly along the grain boundary. Zone IV had the same phase composition as the matrix, but oxide compounds were also observed at the grain boundary.

For the oxygen-saturated liquid lead, the oxide layer grew fast and could research a thickness about 30 μm after 17 h for Fe–16Cr alloy and 20 μm after 13 h for Fe–16Cr–1Al alloy, then exfoliation of the oxide was observed. The oxide film was mainly composed of magnetite in which some oxide particles were found. Lead was also detected in the oxide film.

The experimental results by Fedirko et al. [36,37] also indicated that the oxidation rate as well as the corrosion loss of the alloy decreased with increasing the content of Cr and Al in the alloy.

The experimental results of the steel tested in oxygen contained liquid lead are summarized in Table 6.

3.2. Oxidation of steels in flowing liquid lead

Compared with tests of steel in stagnant liquid lead, tests of steels in flowing liquid lead are scarce. Up to now, to our best knowledge only two references are available (Glasbrenner et al. [38] and Gorynin et al. [29]).

3.2.1. Austenitic 1.4970 and 1.4948 steels

The austenitic steels 1.4970 and 1.4948 were tested at 823 K in a liquid lead loop [38] in which the oxygen concentration was controlled in the range of 0.3–0.4 ppm. The temperature difference of the loop was 150 K and the flow velocity of the liquid was 1.9 m/s.

After 3000 h of exposure, a very thin oxide layer formed on the steel surface (~2 μm) which was found to be protective and could prevent the dissolution attack of the liquid lead at least during the 3000 h of exposure.

If the surface of these austenitic steels was treated by GESA, very different oxide layer structure was formed compared with the one without treated by GESA under the same experimental conditions. Up to 3000 h of exposure, a pretty thick (~45 μm for 1.4948 and 36 μm for 1.4970) duplex oxide layer was observed on the steel surface.

The outer layer was composed of pure magnetite. Other elements like chromium, nickel and lead were not detected in this layer. The inner layer contained iron, chromium, nickel and oxygen, corresponding to an iron–chromium spinel plus nickel. In the inner layer, the concentration of iron and chromium was almost constant, while the concentration of oxygen decreased slowly and the concentration of nickel increased slightly towards the steel side. It was found that the concentration of chromium and nickel in the inner layer was greater than that in the substrate steel. No oxide spallation was reported up to 3000-h test and the oxide layer was expected to be protective.

3.2.2. Ferritic OPTIFE and EM-10 steels

Ferritic OPTIFER and EM-10 steels were also tested in the same liquid lead loop [38]. After 3000 h of exposure, the micrograph showed the typical oxidation attack with three different zones. The layer at top was composed of magnetite without appreciable chromium concentration. The layer in the middle contained Fe–Cr spinel. Underneath the oxide layer, an oxygen diffusion layer was observed in which oxides precipitate along the grain boundaries. The thickness of the duplex oxide layer increases with increasing the time of exposure. No dissolution of the steel components was reported and the oxide layer was expected to be protective.

Unlike with the austenitic steels, GESA treatment had no obvious influence on oxide layer structure as well as on the composition of the oxide layer.

3.2.3. Fe/Cr/Ni/Si alloys

Kinds of Fe/Cr/Ni/Si alloys were tested in a liquid lead loop [29] up to 13,500 h at 823 K. The temperature difference of the loop was 200 K and the flow velocity was in the range of 0.5–3 m/s. The oxygen concentration was controlled in the range of 0.001–1 ppm. The thickness of the oxide layer was found to increase with time as shown in Fig. 8. No more information on the oxide layer structure was reported.

The experimental results of the oxide layer formed in flowing lead are summarized in Table 7.

3.3. Summary experimental results

1. Except for the experiments at 923 K, experiments at other temperatures show that the oxide layer formed on the surface of steels are protective.
2. For ferritic/martenstic steels, the oxide layer always has a duplex-layer structure. For austenitic steels, the oxide layer has single-layer structure if the temperature is below 823 K, while at 823 K, both single-layer and duplex-layer structures were reported in stagnant systems, and only single-layer structure was found in flowing systems.
3. GESA treatment has significant effects on austenitic steels in flowing systems. It not only enhances the oxidation rate but also changes the single-layer structure formed on the steel without GESA treatment to duplex-layer structures. However, GESA treatment has very few effects on austenitic steel in stagnant systems and few effects on ferritic steels in both flowing and stagnant systems.
4. Aluminized treatment can prevent both corrosion and oxidation. Therefore, it is an effective way to enhance the corrosion resistance of steels in liquid lead environments.
5. Oxygen diffusion layer underneath the oxide layer was reported for ferritic steels in both stagnant and flowing systems, but was found for austenitic steels only in stagnant systems.
6. In stagnant systems, metallic lead was found in the oxide layer if the temperature is below 823 K. While, lead exists as oxide compounds at 923 K. No lead was found in the oxide layer in a flowing system.
7. The protective efficiency depends on the oxide composition contacting with the liquid lead. The magnetite layer has a lower protective efficiency compared with the Fe–Cr spinel.

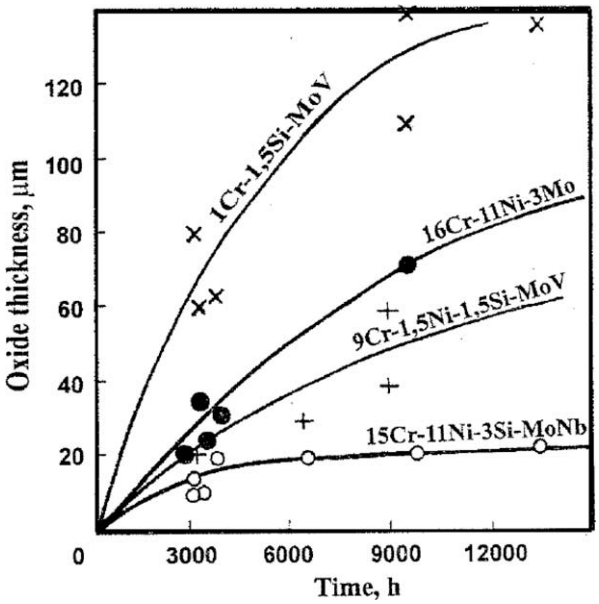

Fig. 8. Oxide growth on steels exposed to flowing lead at 823 K with an oxygen concentration range of 0.001–1 ppm [29].

4. Oxidation of steels in LBE under oxygen controlled

Without protection, lead–bismuth eutectic is more corrosive to common stainless steels than liquid lead under the same operating conditions. Along with the studies on corrosion by liquid lead, there are more studies on corrosion by lead–bismuth eutectic recently, most of which were focus on how to developing the protective oxide layer on steels using for structural materials for LBE systems to enhance to the life time.

4.1. Oxidation of steels in stagnant LBE

4.1.1. AISI 316L steel

This steel was tested 573, 673 and 749 K in stagnant LBE with oxygen saturated [30]. At 573 and 673 K, a very thin oxide layer (<1 μm) formed on the steel surface after 5000 h. At 749 K, the thickness of the oxide layer can research 2–4 μm after 1200 h. The layer has a single structure and was composed of $Fe(Fe_{1-x}Cr_x)_2O_4$.

Experiments were also carried out at 823 K with saturated oxygen [39]. The corrosive behaviour at this temperature was very different from those at lower temperatures. After 1500 h, a thin oxide

Table 7
Summary of the experimental data of steels exposed to flowing liquid lead with oxygen control.

Steel	Temp. (K)	ΔT	Oxygen (ppm)	Velocity (m/s)	Time (h)	Thickness (μm)	Composition
1.4948 GESA	823	150	0.3–0.4	1.9	1027 2000 3027	28 41 45	Duplex structure; outer layer: Fe3O4; inner layer: Fe–Cr spinel.
1.4948	823	150	0.3–0.4	1.9	1027 2000 3027	1.5 1.8 2.0	Single layer
1.4970 GESA	823	150	0.3–0.4	1.9	1027 2000 3027	28 32 34	Duplex structure; outer layer: Fe3O4; inner layer: Fe–Cr spinel.
1.4970	823	150	0.3–0.4	1.9	1027 2000 3027	1.5 1.8 2.0	Single layer
OPTIFER	823	150	0.3–0.4	1.9	1027 2000 3027	36 44 47	Duplex structure; outer layer: Fe3O4; inner layer: Fe–Cr spinel. And oxygen diffusion layer
EM-10	823	150	0.3–0.4	1.9	1027 2000 3027	26 31 34	Duplex structure; outer layer: Fe3O4; inner layer: Fe–Cr spinel. And oxygen diffusion layer
1Cr–1.5Si–MoV	823	200	0.001–1	0.5–3	3000	16–18	
9Cr–1.5Si–MoV	823	200	0.001–1	0.5–3	3000	3.0–24	
16Cr–11Ni–3Mo	823	200	0.001–1	0.5–3	3000	3.0–26	
15Cr–11Ni–3Si–MoNb	823	200	0.001–1	0.5–3	3000 6500 10,000 13,500	3.0–15 17.5 20 22	
9Cr–1.5Ni–1.5Si–MoV	823	200	0.001–1	0.5–3	3000 6500 9000	20 27 39	
16Cr–11Ni–3Mo	823	200	0.001–1	0.5–3	3000 3250 3800 9500	20.0 27.0 32.5 70.00	
1Cr–1.5Si–MoV	823	200	0.001–1	0.5–3	3000 9500 13,500	60–80 110–140 135.00	

scale was found in few areas and the most of the parts of the edge has a spongy appearance as shown in Fig. 9. It was found that spongy layer was mainly composed of Fe and O, and the Cr and Ni content in this layer was about 5 and 2 wt.%, respectively, which is much less than the original content in the steel. After 3000 h, Pb and Bi were found underneath the spongy layer. The corrosion mechanisms at this temperature were the dissolution of the steel components and the penetration of the liquid metal. It was expected that the deepness of liquid metal penetration increases with increasing the time of exposure.

Another test at 823 K with oxygen saturated was carried by Gnecco et al. [40]. After 550 and 1000 h, a two-phase oxide scale composed of magnetite and a spinel zone underneath with a thickness about 7–8 μm was found on the steel surface. The spinel layer was found to be $Fe(Fe_{1-x}Cr_x)_2O_4$ plus nickel. In some areas, lead and bismuth were found in the magnetite layer. At the same temperature while reducing the oxygen concentration to 3.9×10^{-5} ppm, liquid attack was observed after 550 h and the liquid penetration layer could reach 60 μm after 2000 h. In the whole penetration zone, nickel and chrome was depleted (Ni: <1 at.% and Cr: <10 at.%).

At 873 K with oxygen concentration of 4.7 ppm, a duplex-layer oxide film was developed on the surface in a static LBE [41]. In general, the oxide film is homogeneous and compact with a very high chromium content (~40%) and molybdenum enrichment (6–11%) in the spinel layer. No nickel participation was observed in the oxide, while the nickel was enriched in the layer beneath the oxide

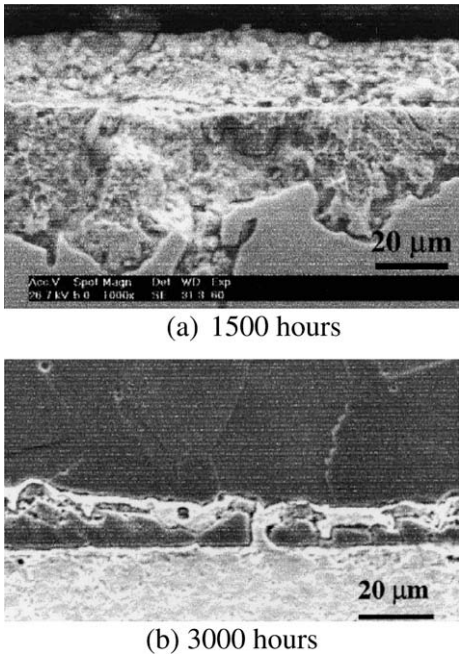

Fig. 9. Cross-section of 316L steel exposed to static LBE with oxygen saturated at 823 K [39].

film up to ~24%. Reducing the oxygen concentration to a value of 0.008 ppm, the steel suffered a slight dissolution after 500 h of exposure. After 1500 h, the liquid metal attack became significant and the attack layer could reach 63 μm.

Keeping H_2/H_2O (0.3 and 0.03) in the cover gas, tests were carried out at different temperatures [42]. At 808 and 823 K, thin oxide layer was formed after 500 h. However, at 873 K no oxide layer was observed and a quite severe dissolution, up to 55 μm was detected. It was also reported that the oxide layer formed at 808 and 823 K after 500 h disappeared after 3000-h testing.

4.1.2. 316 steel

Compared with the 316L steel, the 316 steel has higher carbon content. Such steel was tested at 723 and 823 K in LBE with oxygen saturated [43]. At 723 K, Neither corrosion nor oxidation was observed after 3000 h of exposure obviously. At 823 K after 3000 h, a thin oxide film was formed on the surface, and beneath the oxide layer a ferritic layer was observed due to the deletion of the nickel, indicating that the film cannot protect the dissolution of Ni.

4.1.3. 304L steel

At 723 K and an oxygen concentration of 4.7 ppm, neither oxide nor dissolution of the steel components was observed after 1500 h of exposure. Reducing the oxygen concentration to ~0.0008 ppm, the steel showed minor signs of dissolution after 2400 h of exposure. At 873 K and an oxygen concentration 4.7 ppm, a very thin oxide film (~0.5 μm) was observed after 100 h. After 1500 h, similar oxide film was detected and carbide precipitation at grain boundaries was found [41]. Even the oxygen concentration was reduced to 0.008 ppm, the steel presented an excellent behaviour at 873 K [42].

4.1.4. 410 and 430 steels

The behaviours of 410 and 430 steels in LBE with oxygen saturated at 723 K and 823 K were similar [43]. The oxide formed on the surface was composed of Fe–Cr oxide and the Cr content in the oxide was about 12%. No decrease in Cr and Fe concentration near the surface region was observed.

4.1.5. F82H steel

Mod. F82H steel was tested at 749 K in stagnant LBE with oxygen saturated [30]. Duplex oxide layer structure was observed after 700 h of exposure. The outer layer, mainly composed of Fe_3O_4, had columnar morphology. Lead was also found in the layer. The inner layer, composed of $Fe(Fe_{1-x}Cr_x)_2O_4$, was more compact and no lead was found in the inner layer. The thickness of oxide layer was 18 and 34 μm after 700 and 1200 h exposure, respectively, which was thicker than the steel in liquid lead under the same operating condition.

Short-term (500 h) tests [44] were carried out for this steel at 808 and 823 K. At 808 K and an oxygen concentration of 0.003 ppm, a duplex-layer oxide film was formed on the steel surface after 500 h. The outer layer, mainly composed of Fe oxide was porous and brittle, and spallation of the most of the outer layer was observed. The inner layer, in where Cr was enriched, was composed of Fe–Cr spinel. Underneath the duplex oxide layer, cavities parallel to the specimen edges, apparently formed by the agglomeration of pores were detected. In some areas, the internal oxide layer was detached and lead–bismuth was observed between the oxide and steel. At 823 K and an oxygen concentration of 0.004 ppm, the steel underwent a corrosion process instead of the oxidation process. A heterogeneous behaviour among the specimens tested at such operating conditions was observed. Some of them showed dissolution with chromium depletion whereas in others non-protective oxide layers and dissolution areas with significant chromium enrichment and iron depletion were detected.

Another experiment at 823 K in LBE with oxygen saturated indicated that there was grain boundary corrosion beneath the oxide film [43].

At 873 K with an oxygen concentration of 4.7 ppm, duplex-layer oxide filmed was formed after 100 h. Chromium enrichment as well as the presence of tungsten was observed in the spinel layer. At the same temperature while reducing the oxygen concentration to a value of 0.0008 ppm, slight dissolution was observed after 1500 h of exposure and chromium depletion was detected below the dissolution zone, while at 723 K and 0.0008 ppm oxygen, no significant corrosion was observed after 2400 h of exposure [41].

4.1.6. EM-10 steel

At 723 K and an oxygen concentration of 4.7 ppm, an oxide layer covering the entire surface was developed after 500 h of exposure. Increasing the temperature to 873 K, the oxide layer became thicker and has a duplex-layer structure. It appeared quite homogeneous and followed a linear law with time after an incubation period. Decreasing the oxygen concentration to a value of 0.0008 ppm, no signs of corrosion were observed at 723 K after 2400 h, while slight dissolution was observed at 873 K after 1500 h [41].

4.1.7. JPCA steel

At 723 K, the thin Fe–Cr oxide film formed on the surface of JPCA steel in a static LBE with oxygen controlled seemed to be protective [43]. No decrease in Cr, Ni and Fe concentrations at the surface area was observed. While at 823 K, a ferritic layer with excessive decrease in Ni and Cr concentration was formed beneath the oxide film.

4.1.8. MANET II steel

This steel was tested at 573, 673 and 749 K in stagnant LBE with oxygen saturated [30]. At 573 K, the steel did not suffer corrosion attack and a very thin oxide layer (<1 μm) could be observed after 5000 h. At 673 K, duplex oxide layer with a thickness about 1 μm was observed after 1500 h and the thickness increased to 5 μm after 5000 h. Similar phenomena were found at 749 K, but the oxide layer became thicker. After 700 h, the thickness was about 11 μm and increased to 16 μm after 1500 h. For the duplex oxide layer, the inner layer was composed of $Fe(Fe_{1-x}Cr_x)_2O_4$ and the outer layer of Fe_3O_4. At 823 K in stagnant LBE with oxygen saturated, inter- and trans-granular attack of the liquid metal was observed after 1500 h. Besides the liquid metal penetration, a thin oxide layer composed of iron, chromium and oxygen was also detected in some area. By increasing the testing time to 3000 and 5000 h, the penetration of the liquid metal became more severe.

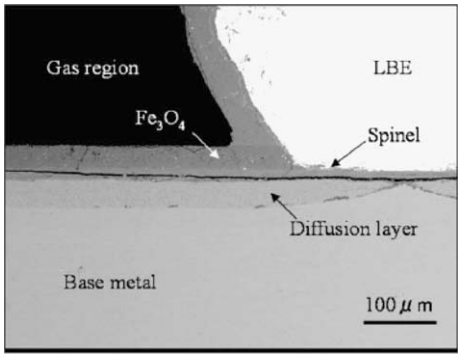

Fig. 10. Cross-section of ODS-M steel through the surface regions of static LBE containing 0.01 ppm at 823 K for 5000 h [45].

4.1.9. SX steel

Such steel has about 5% Si. At 823 K, a very thin (0.2–0.4 μm) oxide film was formed after 3000 h exposure to LBE with oxygen saturated [43]. The film was an oxide composed of Si and O. Enrichment of Cr, Fe and Ni was not found. It was found this film was very protective because it prevents dissolution of Ni and Cr significantly.

4.1.10. T-91 steel

Such steel was tested at 873 and 723 K in static LBE with different oxygen concentrations [41]. At 873 K and an oxygen concentration of 4.7 ppm, a quiet homogeneous duplex-layer structure and thick oxide layer was formed. In the spinel layer, the chromium and molybdenum were significant enriched. When reducing the oxygen concentration to 0.0008 ppm, corrosion attack was observed and the attack depth could reach 13 μm after 1500 h of exposure. At 723 K and an oxygen concentration of 4.7 ppm, a thin oxide film was developed after 500 h and the thin film covered the entire surface. When the oxygen concentration was reduced to 0.0008 ppm, no sign of corrosion was observed after 2400 h of exposure.

At 823 K with saturated oxygen, duplex-layer oxide layer was found after 550 and 1000 h [40] with a thickness of 7 and 12 μm, respectively. It was reported that the outer layer was not pure magnetite but containing 9 at.% Cr. An oxygen diffusion zone was found underneath the oxide layer. In the oxygen diffusion zone, spinel oxide was observed along the grain boundaries. At the same temperature while reducing the oxygen concentration to 0.39 ppm, intergrannular was found after 550 h and the liquid penetration could reach 30 μm after 2000 h.

4.1.11. ODS-M steel

Exposure tests of an ODS-M (oxide dispersion strengthened martensitic) steel were performed in stagnant LBE at different temperatures and oxygen levels [45]. An example of the cross-section view after 5000 h of exposure to LBE containing 0.01 ppm oxygen at 823 K is given in Fig. 10. The figure indicates that the oxide layer in LBE is much thinner than that in gas. The author thought that the outer layer of the oxide layer formed in LBE spalled off which resulted in a thin oxide layer. It was also reported that the thickness of the spinel layer is almost the same in the atmosphere and LBE. At the same oxygen level while increasing the temperature to 873 and 923 K, A thin Fe–Cr spinel oxide was observed that could partially protect the steel up to 2000 h, and after 5000 h the protective layer disappeared partly but after 10,000 h the layer disappeared completely with the consequence of an overall dissolution.

At an oxygen concentration of 10^{-4} ppm, a thin protective Fe–Cr spinel oxide layer was formed completely covering the steel surface up to 2000 h at 923 K. Only in a few places, LBE penetrated through the oxide scale into small pores below the surface. Increasing the oxygen concentration to 1 ppm resulted in very different behaviour from the low oxygen concentrations. Duplex-structure oxide layer was formed and the layer broke off between 2000 and 5000 h of exposure, and a renew scale was observed after 5000 h.

The oxidation behaviour of steels in stagnant LBE with containing oxygen is summarized in Table 8.

4.2. Oxidation of steels in flowing LBE

Most of the experimental studies on corrosion by liquid LBE were carried out in non-isothermal flowing systems to mimic the conditions of a nuclear coolant system in advanced nuclear reactors.

4.2.1. AISI 316L steel

Neither corrosion nor oxidation attack was observed at the cold test section (573 K) and hot test section (743 K) after 3000 h in the CU-1M loop in which the flow velocity was 1.9 m/s and the oxygen concentration was controlled in a range of 0.01–0.02 ppm [46]. In the same loop while increasing the temperature to 733 K at the cold test section and 823 K at the hot test section and the oxygen concentration to a range of 0.03–0.05 ppm, very different corrosion

Table 8
Summary of the experimental results of steel tested in static LBE with oxygen control.

Steel	Temp. (K)	Oxygen (ppm)	Time (h)	Thickness (μm)	Description
AISI 316L	573	Saturated	5000	<1	Single layer: $Fe(Fe_{1-x}Cr_x)_2O_4$
	673	Saturated	5000	<1	Single layer: $Fe(Fe_{1-x}Cr_x)_2O_4$
	749	Saturated	1200	2–4	Single layer: $Fe(Fe_{1-x}Cr_x)_2O_4$
	823	Saturated	1500	Very thin	In few areas: very thin oxide, liquid metal penetration
			3000	Very thin	
	823	Saturated	550	7–8	Outer layer: Fe_3O_4, Inner layer: $Fe(Fe_{1-x}Cr_x)_2O_4$ + Ni
			1000	7–8	
316	723	Saturated	3000	–	No corrosion and oxidation
	823	Saturated	3000	Very thin	Ferric layer formation
304L	723	4.7	1500	–	Minor dissolution for the lower oxygen concentration
		0.0008	2400	–	
	873	4.7	100	<1	Carbide precipitation
		0.008	1500		Excellent behaviour
F82H	749	Saturated	700	18	Outer layer: Fe_3O_4 + Pb, Inner layer: $Fe(Fe_{1-x}Cr_x)_2O_4$
			1200	34	
MANET II	573	Saturated	5000	<1	
	673	Saturated	1500	1	Outer layer: Fe_3O_4, Inner layer: $Fe(Fe_{1-x}Cr_x)_2O_4$.
			5000	5	
	749	Saturated	700	11	Outer layer: Fe_3O_4, Inner layer: $Fe(Fe_{1-x}Cr_x)_2O_4$.
			1200	16	
	823	Saturated	1500	Very thin	Liquid metal penetration
			3000	Very thin	
			5000	Very thin	
T-91	823	Saturated	550	7	
			1000	12	

behaviour was observed [47]. At the cold test section, a pretty thin oxide layer (<1 μm for the time less than 2000 h and ~1 μm for the time 3000 h) was formed. The thin oxide layer was not protective and slot corrosion was detected on the steel surface after 2000 h. The maximal depth of the slot was about 60 μm. At the hot test section, only small piece of oxide layer was detected and local liquid metal corrosion could reach a value of 220 μm.

Neither component dissolution nor corrosion [48] was found at 693 K after tested of 5000 h at a condition with a flow velocity of 2 m/s and an oxygen concentration of 0.01 ppm. In the same loop, at the hot test section (873 K) deep liquid metal penetration and massive ablation of the material by erosion was observed as shown in Fig. 11. As reported by the authors, the penetration zone is depleted in Ni down to 1 at.%. Spallation was found at 823 K with an oxygen concentration of 0.01 ppm after 7200-h exposure [49]. If the steel surface is treated by wrapping Al-foil and heating at 1313 K for 0.5 hour, the steel showed good corrosion resistance even at 873 K. While if the surface was treated by hot-dipping aluminization and annealing, severe attack and penetration of the liquid metal was observed even at 693 K. Similar attack was also found at temperate 673 K in the LECOR loop with a flow velocity 3 m/s and an oxygen concentration $<7.3\times10^{-4}$ ppm [50] after tested 1500 h. In the same loop while increasing the temperature to 723 K, a corrosion process based on elemental dissolution has been found to be started [51] after 1000-h exposure.

A very thin protective oxide layer was formed after 1000-h exposure at 643 K for both 0.01 ppm and 0.001 ppm oxygen levels with a flow velocity 1.9 m/s. While for the same condition at a higher temperature 873 K, severe dissolution was observed for the low oxygen concentration (0.001 ppm), and severe oxidation was found at the high oxygen level (0.01 ppm). For both oxygen levels, flow-induced erosion was observed [52]. While if the surface of the steel was coated by aluminum, the steel shows good corrosion resistance at 873 K for the oxygen levels [53].

4.2.2. 316 steel

When the oxygen concentration is low, the dissolution corrosion of 316 steel is severe. For example, the corrosion rate is in the range of 0.4–1.5 mm/yr at 773 K [54]. While no dissolution corrosion was observed after tested 3000 h in CU-1M loop at the cold (733 K) and hot (823 K) test sections [47] with an oxygen concentration of 0.03–0.05 ppm and a flow velocity 1.9 m/s. At the cold test section, the protective oxide layer has a single-layer structure, while at the hot test section the layer has a duplex-layer structure with outer layer was composed of magnetite and inter layer was composed of Fe–Cr spinel. The layer became thicker with exposure time.

Liquid metal penetration was observed at low oxygen levels [55]. At 823 K and with a velocity of 2 m/s, it was reported that Pb penetrated into a depth of approximately 42 μm in the outer region, while Pb–Bi penetrated into the depth of 208 μm in the intermediate region after 1000-h exposure to LBE with an oxygen concentration of 2.0×10^{-5} ppm.

4.2.3. 1.4790 steel

Similar to 316 and 316L steels, 1.4790 steel has a high corrosion resistance at lower temperature such as 573 and 743 K. No dissolution corrosion or oxidation [46] was observed after 3000-h exposure to LBE with an oxygen concentration of 0.01 ppm because of a very thin protective oxide layer [56]. By increasing the temperature to 823 and 873 K, both duplex- and single- structure oxide layer were observed after 2000-h exposure [48]. Precipitation of chromium oxide was found in the grain boundaries of the spinel oxide zone represented by the dark network in Fig. 12. If the steel surface was alloyed by Al-foil wrapping, no dissolution attack or liquid metal penetration was visible even at 873 K, while the dissolution corrosion could be accelerated by treating the steel surface through alloying the steel by Al-hot dipping.

Long-term tests up to 7200 h at an oxygen level of 0.01 ppm indicate that the duplex oxide layer formed at 823 K is protective although oxide layer spallation was found and replaced by new protective one, while at 873 K severe attack was found after 2000 h [49].

4.2.4. D-9 steel

At a test condition with an oxygen concentration 0.03–0.05 ppm and a flow velocity of 1.9 m/s, the behaviour of D-9 steel in flowing LBE is similar to these of 316 steel [47]. At 733 K, the thin protective oxide layer could reach 2–6 μm after 3000 h. At 823 K, duplex-structure oxide layer with a thickness in the range of 2–36 μm was found after 2000 h and the thickness increased to 40 μm after 3000 h. Both the duplex and single-structure oxide layers are protective up to 3000-h exposure.

4.2.5. 304, 304L and 321 steels

Tests on these steels by Ilincev et al. [54] indicate that the corrosion rate of 304 and 304L steel ranges from 0 to 800–1200 μm/yr depending on whether the surface of the specimen had been passivated or grounded. The corrosion rate of 321 steel does not exceed 30–40 μm/yr. Considering that 321 steel has Ti compared with 304 steel, the corrosion rate may be reduced by the presence of Ti. If 2% Si was added to the steels, no corrosion was detected.

In the same test, specimens of 316 steel with a ground surface have a corrosion rate in the range of 400–1500 μm/yr.

4.2.6. HT-9 steel

At a test condition with an oxygen concentration of 0.03–0.05 ppm and a flow velocity of 1.9 m/s, non liquid metal corrosion was observed and a duplex-layer oxide layer was formed on the steel surface at 733 and 823 K up to 3000 h [47]. At 733 K, the thickness of the oxide layer was 1–8, 12–14 and 14–16 μm after 1000, 2000 and 3000 h, while the thickness at 823 K, was 8, 32–36 and 38 μm, respectively. The oxide layer is pretty uniform.

4.2.7. T-91 steel

At 573 K, very thin oxide layer was formed up to 3000 h for a tested condition with an oxygen concentration of 0.01 ppm and a flow velocity of 1.9 m/s. The layer became to a duplex structure

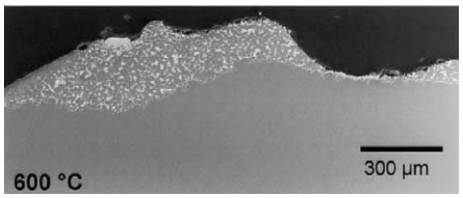

Fig. 11. Cross-section of AISI 316L after tested of 2000 h in flowing LBE at 873 K and 0.01 ppm oxygen. Bright inclusions consist of Pb/Bi alloy enriched in Bi [48].

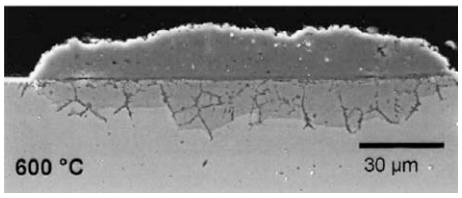

Fig. 12. Cross-section of 1.4790 steel after 2000 h in flowing LBE at 823 K and 0.01 ppm oxygen [48].

at the temperature 743 K. The thickness of the oxide layer is 11, 14 and 16 after 1000, 2000 and 3000 h of exposure [46,56]. At 873 K, weight losses were found and a thick oxide layer was observed after 1000 h (20–25 μm). The oxide layer was composed of three layers, and the outer layer, unlike the duplex oxide layer was not composed of magnetite but Fe–Cr spinel. The internal layer was an oxygen diffusion layer where the oxygen concentration progressively decreases to zero. The intermediate layer is locally observed. It is porous and heterogeneous and appears enriched in chromium and oxygen with low iron content [52]. Reducing the oxygen concentration to 0.001–0.0001 ppm, weight losses were measured as well as oxide layer was observed after 1000 h of exposure at both temperature 743 and 873 K. The layer was 10–15 μm at 873 K. Liquid metal penetration and cavities at the surface [50] was found when the oxygen concentration was at the round of 3.1×10^{-6} ppm at 673 K.

4.2.8. T-410 steel

At a condition with an oxygen concentration of 0.03–0.05 ppm and a flow velocity 1.9 m/s, the steel was subjected to heavy liquid metal corrosion even at the lower temperature 733 K after 2000 h of exposure [47]. The oxide was neither uniform nor continuous. No duplex-layer oxide structure was observed at 823 K.

4.2.9. 405 and 430 steels

At 823 K, duplex oxide layer was observed after 1000 h of exposure to a condition [57] with an oxygen concentration of 17×10^{-4} and 3.7×10^{-4} ppm and a flow velocity of 1 m/s.

4.2.10. MANET steels

Such steel is designed for lower temperature applications. Under a condition with an oxygen concentration of 0.01 ppm and a flow velocity of 2 m/s, thick oxide layer with a duplex-layer structure was developed during 2000-h tests at 693 and 823 K [48]. At 823 K, the magnetite layer spalls off between 2000 and 4000 h and also part of the spinel layer. A thin oxide layer and at some places a thicker one which replace the spalltion one again protects the surface [49].

4.2.11. F82H steels>

Through bubbling gas with 10 ppm oxygen at the hot section to control the oxygen concentration, Briceno et al. [58] reported that duplex-layer oxide formed on the steel surface at 823 K. The inner layer was composed of $Fe(Fe_{2-x}Cr_x)O_4$ and the outer layer was composed of magnetite. Up to 3000 h, the oxide layer was found to be protective. At a lower oxygen concentration (2×10^{-5} ppm), Kondo et al. [57] found liquid metal penetration into grain boundary with a depth up to 22 μm after 1000 h at 823 K with a flow velocity of 1 m/s. Some vacancies were also observed around the interface between the Pb–Bi penetration region and the steel matrix.

4.2.12. EM-10 steel

At a condition with an oxygen concentration of 0.01 ppm and a flow velocity of 2 m/s, a thin oxide scale was found but not uniformly distributed, and there was no dissolution corrosion at 573 K. At 743 K, duplex oxide layer was formed and the thickness is 15, 17 and 22 μm after 1000, 2000 and 3000 h [46,56]. Reducing the oxygen concentration to a value of 0.001–0.0001 ppm, although an oxide layer with a thickness of 5–10 μm was formed on the surface after 970 h, small weight losses were measured. At 873 K, dissolution corrosion was clear even at a higher oxygen concentration (0.01 ppm) [52].

4.2.13. EP823 steel

Compared with other martensitic steels such as T-91 and EM-10, EP823 steel has high resistance to both liquid metal corrosion and oxidation. At the same condition, the oxide layer formed on EP823 is much thinner than that on T-19 and EM-10, but more protective [46].

4.2.14. Batman 27 (BA27) and 28 (BA28) steels

At a low temperature (573 K) with an oxygen concentration of 0.01 ppm, the steel was covered with a thin oxide layer after 1000 h of exposure and the thin oxide layer was protective. At 743 K, a duplex oxide was formed. The average thickness measured on Batman 27 was 10, 13 and 15 μm after 1000, 2000 and 3000 h, respectively, and on Batman 28 the thickness was 12, 15, and 17 μm. The duplex oxide layer was found to be protective [46].

4.2.15. OPTIFER IVc steel

Such steel has similar behaviour in flowing LBE to T-91 with the exception that the thickness of the oxide layer is much larger at the same conditions. For example, at 743 K with an oxygen concentration of 0.01 ppm and a flow velocity of 1.9 m/s, the thickness of the oxide layer varies from 16 μm for an exposure time of 1000 h to 22 μm for 3000 h [46,56].

4.6. Summary on oxidation of steels in flowing LBE

1. At a low oxygen concentration (<10^{-4} ppm), both austenitic and martensitic steels are subjected to liquid metal corrosion due to dissolution of the steel components.
2. For Austenitic steel, very thin oxide layer composed of Fe–Cr spinel is formed if the temperature is lower than 773 K. The thin oxide layer was reported to be protective.
3. If the temperature is above 773 K, duplex-layer or single-layer oxide film may be formed. For the duplex structure, it was found that the outer layer was mainly composed of magnetite and the inner layer was composed of Fe–Cr spinel plus nickel. The duplex-layer oxide film is protective at higher temperature, while single-layer film is not protective at least for 316L stainless steel.
4. For austenitic steels, ferritic layer can be formed underneath the protective layer.
5. For martensitic steels, duplex-layer oxide film can be formed on the steel surface. The film can protect the steel from dissolution. While with increasing the temperature, the oxide layer becomes thicker and may spall off.
6. For ODS steels, thicker duplex-layer oxide film is formed if the oxygen is high (>0.01 ppm) and the magnetite layer can spall off with time, and thin single-layer oxide film is formed which is protective up to 923 K if the oxygen concentration is low (~0.0001 ppm).

Table 9
Fitted oxidation constant and the corrosion rate for vary of steels in flowing liquid lead at 823 K with a flow velocity of 1.9 m/s and an oxygen concentration of 0.3–0.4 ppm (data from Ref. [38]).

Steel	$k_p \times 10^{17}$ (m²/s)	R_C		δ_{ss} (μm)
		$\times 10^{12}$ (m/s)	mm/yr	
1.4790	0.1	0.15	0.0035	3.33
1.4748	0.1	0.15	0.0035	3.33
1.4790 by GESA	40.8	4.5	0.105	45.0
1.4748 by GESA	29.2	1.5	0.035	97.5
OPTIFER	62.5	4.5	0.105	69.0
EM-10	31.7	3.0	0.070	52.8

7. Increasing the content of Si in the steel can enhance both the corrosion and oxidation resistance.
8. Among the austenitic steels considered, 304L appears to be the type having the highest resistance to both corrosion and oxidation. Among the marstenitic steels considered, EP823 appears to be the type.
9. Between 823 and 873 K, there is a threshold temperature above which no protective oxide film can be formed and the steel (marstenitic and austenitic) is subjected liquid metal corrosion.
10. In some experiments, LBE was found in the magnetite layer when the temperature is high.
11. In a flowing system, erosion was reported for 316L, while no such phenomenon was observed for 316 tested at the same conditions.
12. If the steel surface was alloyed by Al-foil wrapping, the oxidation and dissolution resistance can be enhanced even at a high temperature such as 873 K. while the steel dissolution is accelerated by treating the steel surface through alloying the steel by Al-hot dipping.

5. Analysis of the experimental data using the oxidation–corrosion interaction model

5.1. Oxidation–corrosion interaction model

The oxidation mechanisms of steels in oxygen controlled liquid lead and LBE systems were recently reviewed by Zhang and Li [2]. Briefly, there are two competitive processes proceeding simultaneously at solid/liquid interface: oxidation and dissolution. Therefore, the growth of oxide layer in liquid metal follows a very different time dependent function compared with that in gas. The Tedmon model [59] for the oxidation process with evaporation was applied to govern the oxidation–corrosion interaction in liquid lead/LBE [60]. The model was rewritten in the following form:

$$\frac{d\delta}{dt} = K_O - R_C, \tag{2}$$

where δ is the thickness of the oxide layer and t is the time, K_O and R_C are the oxide layer growth rate and oxide removal rate by the liquid metal, respectively. For parabolic law, the oxide growth rate can be expressed:

$$K_O = \frac{k_p}{2\delta}, \tag{3}$$

where k_p is the parabolic constant. The removal rate decreases in time for a stagnant liquid lead/LBE because the concentration of corrosion product approaches its solubility level. For a flowing system, especially for a non-isothermal loop system such as the coolant loop of a nuclear reactor, the scale removal rate can be treated as constant if the flow is fully turbulent flow and at steady state.

For the parabolic oxidation rate and the constant scale removal rate, an approximate solution was obtained for short term [60]:

$$\delta = (2R_C\delta_s t)^{1/2} - \frac{2}{3}R_C t. \tag{4}$$

The steady state thickness δ_s is defined by:

$$\delta_s = \frac{k_p}{2R_C}, \tag{5}$$

Knowing the oxide layer thickness and the corresponding time, the oxidation rate and the corrosion rate or the scale removal rate can be obtained by Eq. (4).

5.2. Oxidation and corrosion rate

The experimental data of kinds of steels in flowing liquid lead were fitted by applying Eq. (4). The results (k_p and R_C) are given in Table 9 and the corresponding comparisons between the fitted curves and the experimental data points are shown in Fig. 13. Clearly, the experimental data follows Eq. (4) very well.

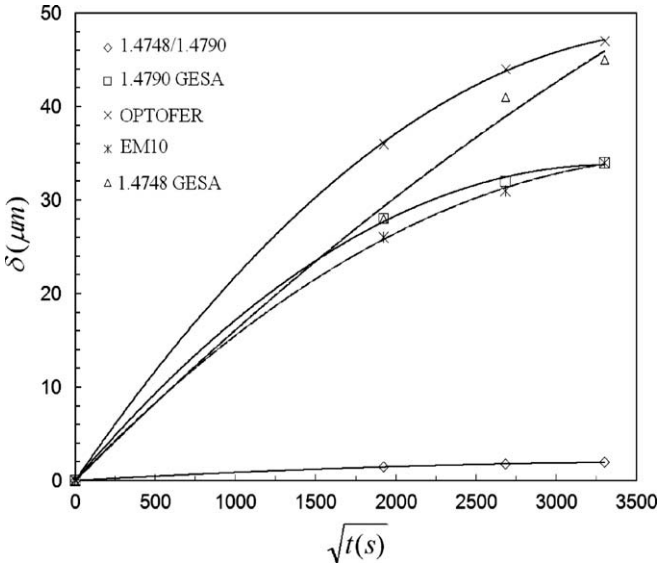

Fig. 13. Comparisons between fitting results (lines) and experimental data (symbols) in flowing liquid lead at 823 K with a flow velocity of 1.9 m/s and an oxygen concentration of 0.3–0.4 ppm.

Table 10
Fitted oxidation constants and corrosion rate for several steels in flowing LBE for different test conditions.

Steel	T (K)	T (K)	V (m/s)	Oxygen (ppm)	k_p $\times 10^{17}$ m^2/s	R_C		δ_{ss} (μm)	Ref.
						$\times 10^{12}$ m/s	mm/yr		
T-91	743	210	1.9	0.01–0.02	5.043	1.052	0.033	23.9	[46,56]
OPTIFER	743	210	1.9	0.01–0.02	10.51	1.781	0.056	29.5	[46,56]
EP823	743	210	1.9	0.01–0.02	1.124	0.1572	0.0049	35.8	[46,56]
BA27	743	210	1.9	0.01–0.02	3.72	0.75	0.0236	24.8	[46]
BA28	743	210	1.9	0.01–0.02	3.048	0.1639	0.0052	93.0	[46]
EM-10	743	210	1.9	0.01–0.02	6.143	0.2942	0.0093	104.4	[46]
316	823	–	0.5	0.01	10.36	1.523	0.048	34.0	[48,49]
1.4790	823	–	0.5	0.01	15.62	1.374	0.043	56.9	[48,49]
HT-9	733	300	1.9	0.02–0.03	3.754	0.3546	0.011	52.9	[47]
HT-9	823	300	1.9	0.02–0.03	14.8	1.01	0.031	73.2	[47]
D-9	823	300	1.9	0.02–0.03	6.87	0.704	0.022	49.0	[47]

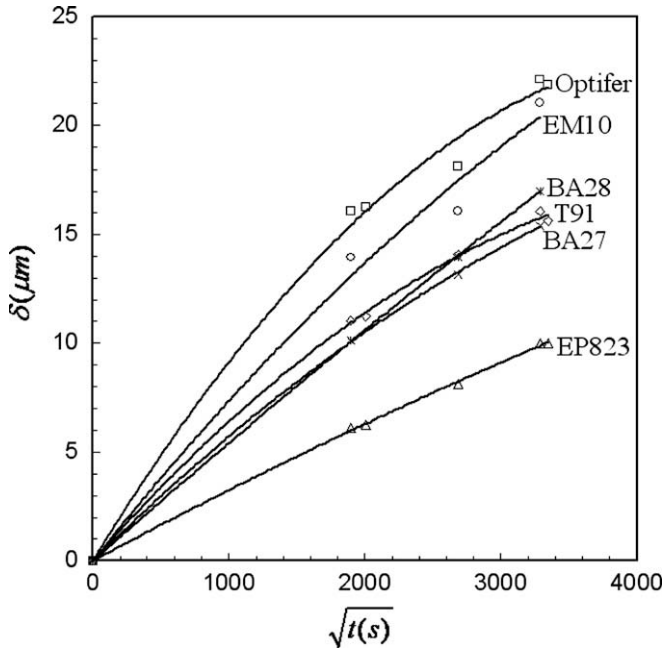

Fig. 14. Comparisons between the fitting results (lines) and experimental results (symbols) in flowing LBE at 743 K with a velocity of 1.9 m/s and an oxygen concentration of 0.01–0.02 ppm.

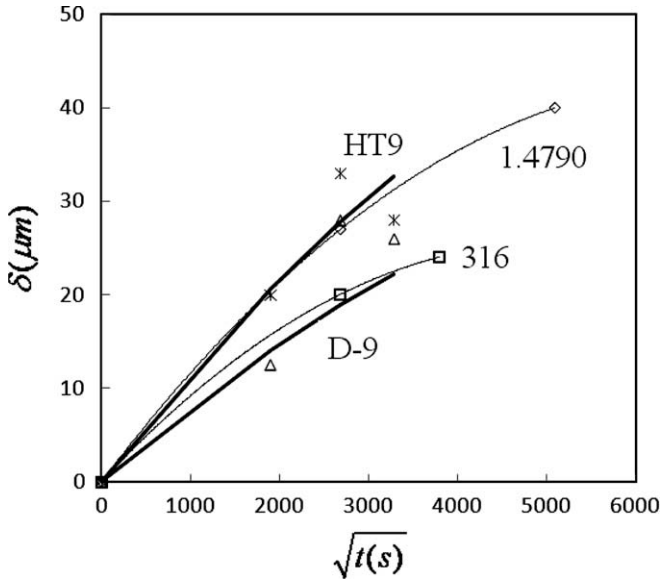

Fig. 15. Comparisons between the fitting results (lines) and experimental results (symbols) in flowing LBE at 823 K of the steels given in Table 10.

Taking into account that all the samples shown in Table 9 were tested under the same operating conditions, the scale removal rate, which only depends on the operating conditions and the oxide layer composition, should be very similar if the oxide contacting with lead has the same compositions despite of the steel compositions. This is true as shown in the table. For the austenitic steel treated by GESA and the ferritic steels, the oxide layer contacting with liquid lead is magnetite, resulting in a very similar scale removal rate. Based on the table, the magnetite layer is less protective than the spinel layer formed on the untreated austenitic steel. The treatment by GESA of the austenitic steel has significant effects on both the oxidation rate and the corrosion rate, and leads to higher values of oxidation and corrosion rate. The oxidation rate constant for ferritic steels are much greater than that for austenitic steels if the steel is not treated by GESA. It is still impossible to develop any correlation with oxygen content and flow rate based on the current experimental data of steels in flowing liquid lead.

Compared with flowing liquid lead, more experimental data is available for flowing LBE. Some experimental results (not all the experimental results reviewed in the present study) are analyzed by using Eq. (4) and the results are given in Table 10 and Figs. 14 and 15. The results in Table 10 for steels of T-91, OPTIFER and EP823 are a little different from the results given in Ref. [60], which is because more data were analyzed in the present study. The re-

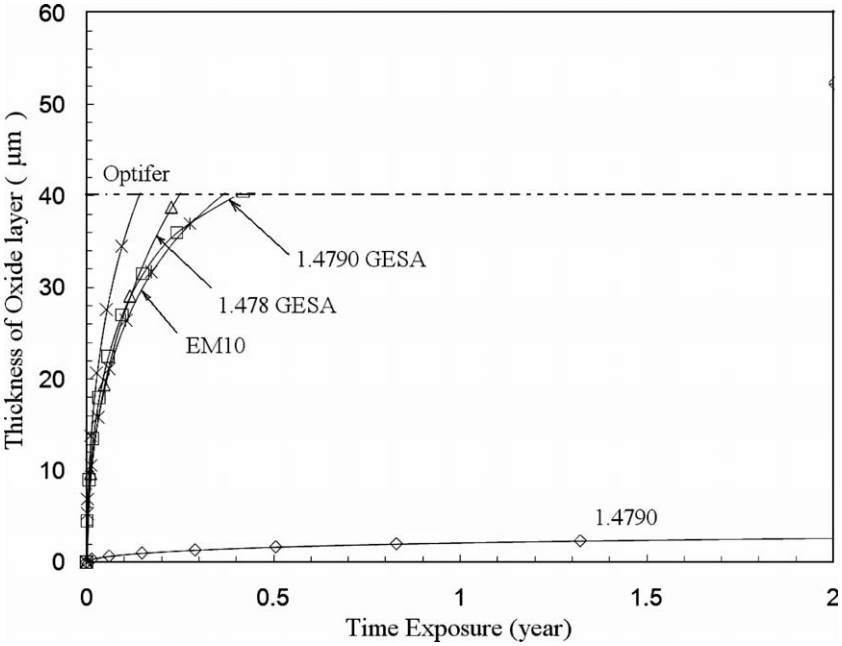

Fig. 16. Long-term behaviour of steels given in Table 9 in a flowing liquid lead with a flow velocity of 1.9 m/s and an oxygen concentration of 03–0.4 ppm at 823 K.

sults for steels of D-9 and HT-9 at 823 K were obtained from Ref. [61].

The figures show that the protective oxide layers obey the law given by Eq. (4) very well at 743 K, but the fitting results by Eq. (4) have some difference between experimental results, especially for steel of D-9 and HT-9, which has been analyzed in Ref. [61]. The oxidation constants are in order of 10^{-17} m/s^2 which is consistent with these in air. The corrosion/scale removal rates at steady state are in the order of 10^{-12} m/s which are similar to those in flowing liquid lead. Considering that the steel surface recession rate depends on the scale removal rate (corrosion rate) only, the larger the corrosion rate, the larger is the surface recession rate.

EP823 steel has the lowest oxidation rate (avoids heavy oxidation) and the lowest corrosion rate (avoids high liquid metal corrosion) compared with other steels in the same condition as shown in Table 10. Therefore such steel seems to be the most suitable one for construal materials of the container for LBE.

The table indicates that the oxidation constant and the corrosion rate are functions of the temperature, flow velocity, oxygen concentration, steel composition and the temperature difference. However, based on the table we cannot get any correlations because of the scarceness of the experimental data.

The calculated thickness of the oxide layer at steady state is also in given Table 10. If the thickness is very large such as the thickness for BA28 and EM-10 at 743 K and HT-9 at 823 K, the steady state cannot be reached because of the spallation. The spallation leads to a sudden high corrosion rate. So these steels are not good materials for a system with flowing LBE.

5.3. Prediction of long-term behaviour and discussion on steel selection

Knowing the oxidation constant and the scale removal rate by fitting available experimental data by Eq. (4), the asymptotic oxide layer thickness or the steady state oxide layer thickness can be calculated using Eq. (5), and the calculated results are shown in Table 9 for liquid lead and Table 10 for LBE. If it is assumed that the oxide layer becomes unstable when the oxide layer exceeds 40 μm, the corrosion–oxidation process cannot reach the steady state because spallation may occur periodically. If the thickness reaches its asymptotic value, the recession rate or the corrosion rate of the steel is determined by the scale removal rate which is a function of the flow conditions and the compositions of the oxide contacting with the liquids.

A relation between the oxide layer thickness and the time was given by Tedmon [59] as:

$$t = \frac{\delta_s}{R_c}[-\theta - \ln(1-\theta)] \tag{6}$$

where θ is the non-dimensional thickness defined by $\theta = \delta/\delta_s$. The curves of the oxide layer thickness as a function of exposure time for several steels given in Table 9 for liquid lead and Table 10 for LBE are shown in Figs. 16 and 17, respectively.

In liquid lead at the conditions considered, the OPTIFER, 1.478 (treated by GESA), 1.4790 (treated by GESA) and EM-10 steels reach the spallation thickness very quickly (less than 0.5 yr), which indicates that these steels cannot be selected as the structural materials for flowing liquid lead at 823 K with a flow velocity of 1.9 m/s and an oxygen concentration of 0.3–0.4 ppm.

Compared with other steels under the same condition, steel EP823 has not only the lowest scale removal rate but also the lowest scale growth rate as shown in Fig. 17. It takes about 26 years for EP823 to reach its steady state thickness which is thinner than the spallation thickness. T-91, BA27 and OPTIFER steels also have steady state thickness less than the spallation thickness at 743 K, but the oxide layer growth rate for these steels are much greater than that for EP823. The quick growth of the oxide layer may result in a loose oxide layer and a local stress that leads to poor protection for the substrate. For steel EM-10 and BA28, the oxide layer quickly reaches the spallation limit resulting in a high corrosion rate, thus these two steel cannot be applied to LBE system even at a low temperature 743 K. At 823 K, steels HT-9, 1.4790 and D-9 cannot be selected because they quickly (about one year exposure) reach the spallation thickness. Stainless steel 316 seems to be applicable under the velocity of 0.5 m/s, but at 2 m/s, significant erosion was reported in Ref. [47].

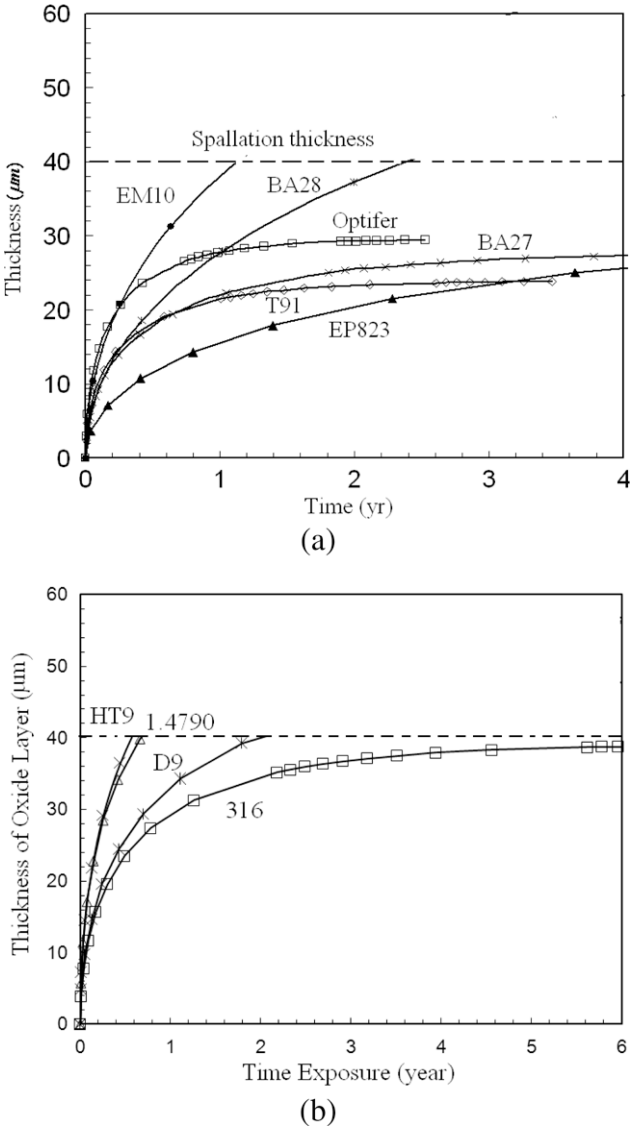

Fig. 17. (a) Long-term behaviour of steels given in Table 10 at 743 K; (b) Long-term behaviour of steels given in Table 10 at 823 K.

6. Discussion

6.1. Oxygen concentration effects

Component distribution in the corrosion layer of steel in flowing liquid lead without oxygen and in the oxide layer of steel in the flowing liquid lead with oxygen [29] is shown in Fig. 18. Clearly, for the case of low oxygen content, significant dissolution

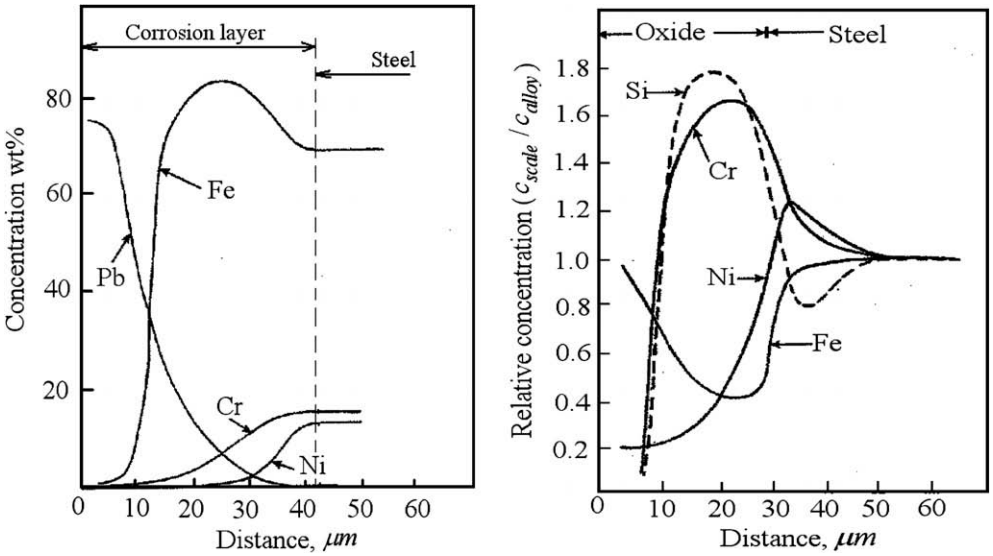

Fig. 18. Composition of corrosion layer on 15Cr–11Ni–3Si–MoNb steel in low content oxygen lead for 2000 h and of the scale on 15Cr–11Ni–3Si–Mo steel exposed to flowing lead for 4000 h at 823 K with oxygen controlled [29].

of the main components of the steel was observed and there is a lead penetration layer. It was reported that typical corrosion damage arises after removing chromium and nickel for austenitic steels [29]. For the case of containing oxygen, no more significant depletion of the steel components in the area underneath the oxide layer, showing the oxide layer is protective. It should be noticed that the oxygen effect on the corrosion by liquid lead/LBE is a function of the oxygen content as indicated by the experimental data. The effect can be classified into three categories [29] as shown in Fig. 5: Corrosion zone, transition zone and oxidation zone. In the corrosion zone, the corrosion rate decreases with the oxygen concentration because of the formation of protective oxide layer. If the oxygen concentration exceeds a certain value as indicated in the figure, high oxidation results in damage of the steel, and in the oxidation zone the corrosion rate or the recession rate of the steel surface increases with oxygen concentration.

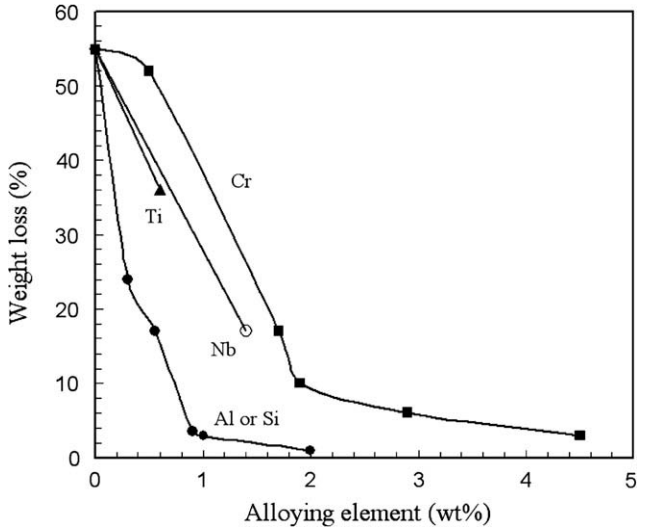

Fig. 19. Effect of alloying elements on low-alloyed steel corrosion in LBE at 873 K and a velocity 6 m/s [29].

6.2. Effects of the steel compositions

At low oxygen concentration, the corrosion rate of steels in LBE depends on the steel composition as shown in Fig. 19 for low-alloy steels [29]. The weight loss decreases with the alloying element Cr, Ti, Nb, Al and Si increasing. Compared with other elements, Al and Si have the most significant effects on increasing the steel corrosion resistance because of the formation of Al/Si oxide film even at low oxygen concentration.

At high oxygen concentration, the thickness of the protective oxide layer also depends on alloying elements as shown in Fig. 20. The thickness decreases as the content of Cr, Si and Ti increases, indicating that the oxidation resistance increases with content of Cr, Si and Ti in the steel. Also, element Si has the most significant effect. It is well known that the oxide film of Si is very compact and protective. Once the oxide film of Si formed, it can prevent the diffusion of other elements and then reduces the oxidation and corrosion rate. A thin protective oxide layer can avoid oxide spallation.

The steel composition also affects the composition and structure of the protective layer. Experimental results indicate that a single-layer oxide film formed on austenitic steels below 773 K is composed of Fe–Cr spinel, while a duplex-layer formed on austenitic steels above 773 K and on martensitic steels for all the temperature considered have a magnetite outer layer and a Fe–Cr spinel inner layer (for example [62]).

The corrosion rate or the scale removal rate at steady state is also a function of the steel composition as shown in Tables 9 and 10. Under the same experimental condition, different types of steel have different corrosion rates. Compared with other martensitic steels shown in the table, EP823 has the smallest corrosion rate. This can be attributed to the high content of Cr and Si in EP823. Because the experimental data are still scarce, it is impossible to obtain any correlation between the corrosion rate and the steel composition of steels in flowing LBE with a protective oxide layer.

6.3. Effects of flow velocity

At steady state, the scale removal rate or the corrosion rate is determined only by the mass transfer rate which depends strongly

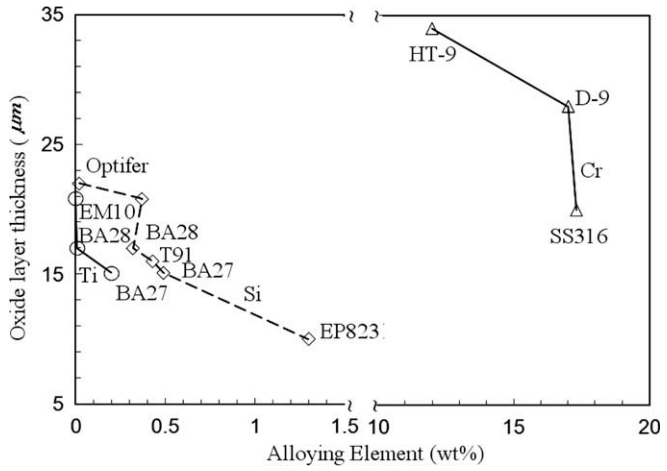

Fig. 20. Examples of effects on the alloys element on the thickness of the oxide layer in flowing LBE [46,47].

on the flow velocity. Based on a corrosion model [2], the corrosion rate is proportional to $V^{0.6-0.8}$ where V is the velocity. Therefore, increasing the flow velocity results in high corrosion rate, while on the other hand, increasing the velocity can lead to compact thin protective oxide layer, preventing the oxide spallation. By optimizing the liquid flow velocity, it is possible to obtain the protective oxide layer with acceptable corrosion rates.

7. Conclusions

This report reviewed and theoretical analyzed the corrosion by liquid lead and lead–bismuth. The following conclusions are obtained:

1. Without protective methods applied, the heavy liquid metals/alloys are very corrosive to stainless steels, low-alloy steels and carbon steels. Only Mo has high corrosion resistance and can be used as the container materials for liquid lead and lead–bismuth.
2. Compared with liquid lead and lead–bismuth, liquid bismuth is more corrosive at the same operation conditions.
3. For metallic inhibitors, the mechanism of inhibition is the formation of protective layer of nitrides or carbides by the chemical reactions between the added inhibitors with the minor elements in the structural materials such as carbon and nitrogen.
4. Zr and Ti are effective metallic inhibitors for carbon steels and low-alloy steels, while for stainless steels the inhibition efficiency is very low.
5. Oxygen is an effective non-metallic inhibitor for stainless steels in liquid lead and lead–bismuth. The inhibition efficiency is affected by the operation conditions such as the oxygen concentration, the flow velocity, temperature, the compositions of the structural materials, etc.
6. When the operating temperature is lower than 773 K, the oxide layer formed on the steel surface by controlling the oxygen concentration in the liquid is protective. The layer may have a single- or double-layer structure, which depends on the substrate steel type.
7. When the temperature is above 823 K, most of the steels considered in this report have a high oxidation rate resulting in a fast growth of the oxide layer. The layer becomes unstable and the oxidation itself becomes a problem. The corrosion rate is also increased by increasing the operating temperature.
8. Among the steels considered, EP823 has the best compatibility with liquid lead and lead–bismuth under oxygen control. At the same operation conditions, EP823 has both lowest oxidation and corrosion rate.
9. If the oxide layer thickness reaches its steady state value in a short term and the steady state thickness is thicker than the defined stable thickness, this oxide layer is not protective for long-term applications because the unexpected spallation results in a higher corrosion rate.
10. Increasing the flow velocity can lead to a thin and compact oxide layer in some cases, however, it can also result in a higher corrosion rate. It is possible to optimize the flow velocity to obtain a compact protective layer with an acceptable corrosion rate for long-term operations.
11. Steel composition plays important roles on both corrosion and oxidation rates. Without inhibitor, the corrosion rate decreases with the content of alloying element Cr, Ti, Nb, Al and Si increasing. With proper oxygen controlled, the protective oxide thickness decreases as the content of Cr, Si and Ti in the steel increasing.

Acknowledgements

The author is grateful to Dr. N. Li at The Los Alamos National Laboratory and Dr. A. Hechanova at The University of Nevada at Las Vegas for the initial support of this study.

Appendix A

Steel composition.

Steel	C (wt.%)	Cr (wt.%)	Ni (wt.%)	W (wt.%)	Mn (wt.%)	Mo (wt.%)	Si (wt.%)	Al (wt.%)	V (wt.%)	Ti (wt.%)	Nb (wt.%)	Ta (ppm)	P (ppm)	S (ppm)	B (ppm)	N (ppm)
1.4948	~0.06	~18	~11		<2.0		<0.75									
1.4970	0.56	16.5	13.8		1.91	0.66	0.89			0.43			120	90		
304	0.08	18–20	8–12		2		1						450	300		
304L	0.03	18–20	8–12		2		1						450	300		
316	0.04	16.83	10.79		1.22	2.06	0.69									
316L	0.02	17.3	12.1		1.8	2.31	0.35					20	190	5	9	74
347	0.08	17–19	9–13		2		1				0.8		450	300		
SUS405		12					1	0.1								
410	0.067	12.21	0.12		0.80	0.02	0.31	0.02	0.07	0.01						0.013
430	0.080	16.24	0.15		0.23	0.02	0.52	0.007	0.10	0.01						0.024
446	0.2	23–27			1.5		1.0						400	200		

Continued on next page

Appendix A (*continued*)

Steel	C (wt.%)	Cr (wt.%)	Ni (wt.%)	W (wt.%)	Mn (wt.%)	Mo (wt.%)	Si (wt.%)	Al (wt.%)	V (wt.%)	Ti (wt.%)	Nb (wt.%)	Ta (ppm)	P (ppm)	S (ppm)	B (ppm)	N (ppm)
20Kh13	0.2	13			<0.8		<0.8									
BA27	0.1	9.0	0.07	1.45	3.1	0.01	0.49		0.21	0.2	0.01					
BA28	0.09	8.94	0.05	1.51	3.51	0.01	0.32		0.24	0.01	0.01					
CRM6	0.09	0.85	0.19		0.48	0.54	0.47									100
Croloy 2-1/4	0.15	2.25				1.0										
D-9		17	12		2		1.0									
EP823	0.18	12	0.8	0.8	0.8	0.9	1.3		0.4		0.4					
EM-10	0.1	8.8	0.2		0.51	1.0	0.37		0.03		0.01					
HT-9		11.5	0.5		0.6		0.4									
Inconel	0.15	15.5	72		1		0.5									
JPCA	0.058	14.41	15.87	0.10	1.54	2.29	0.50	0.012	0.03	0.22						30
F82H	0.09	7.8	0.04	2	0.18	<0.01	0.13		0.16	<0.02	<0.01	200	40	30	<10	60
Mol.F82H	0.09	7.8	0.04	2	0.18		0.13		0.16	0.01	<0.01		40	30	90	60
MANET	0.11	10.3	0.68		0.78	0.61										
MANET II	0.11	10.3	0.68		0.78	0.61			0.20		0.14		30			30
Mod.9Cr–1Mo	0.1	8.41	0.06	0.0005	0.4	0.88	0.3	0.033	0.2	0.01						0.047
OPTIFER IVc	0.56	9.99		0.30	0.58		0.02		0.28			200	50	90		
ODS-M (0.17% O)	0.13	8.85	0.01	1.94	<0.01		<0.005			0.02			10	30		110
SX	0.01	17.58	19.08		0.60	0.356	4.80									
T-91	0.105	8.26	0.13		0.38	0.95	0.43		0.2		0.075					

References

[1] J. Weeks, H.S. Isaacs, Corrosion and deposition of steels and nickel-base alloys in liquid sodium, in: M.G. Fontana, R.W. Staehle (Eds.), Advances in Corrosion Science and Technology, vol. 3, Plenum Press, 1973.

[2] J. Zhang, N. Li, Review of the studies on fundamental issues in LBE corrosion, Journal of Nuclear Materials 373 (2008) 351–377.

[3] Handbook on Lead–bismuth Eutectic Alloy and Lead Properties, Materials Compatibility, thermal-hydraulics and Technologies, 2007 Edition, Nuclear Energy Agency, OECD 2007, NEA No. 6195.

[4] J.V. Cathcart, W.D. Manly, The mass transfer properties of various metals and alloys in liquid lead, Corrosion 12 (1956) 43–47.

[5] W.D. Manly, Fundamentals of liquid metal corrosion, Corrosion 12 (1956) 46–52.

[6] H. Shimotake, J.C. Hesson, Corrosion by fused salts and heavy liquid metals – a survey, Advances in Chemistry Series 64 (1967) 149–185.

[7] J.J. Park, D.P. Butt, C.A. Beard, Review of liquid metal corrosion issues for potential containment materials for liquid lead and lead-bismuth eutectic spallation targets as a neutron source, Nuclear Engineering and Design 196 (2000) 315–325.

[8] I. Ali-Khan, Corrosion of steels and refractory metals in liquid lead, in: Proc. Internat. Seminar Mat. Behav. Phys. Chem. Liq. Met. Systems (Carlsruhe 1982), Plenum, New York, 1982, pp. 243–252.

[9] J. Sannier, G. Santarini, Corrosion two ferritic steels by liquid lead circulated in a thermosypon, finding of model, Journal of Nuclear Materials 107 (1982) 196–217.

[10] R.C. Asher, D. Davies, S.A. Beetham, Some observations on the compatibility of structural materials with molten lead, Corrosion Science 17 (1977) 545–557.

[11] J.A. James, J. Trotman, Corrosion of steels in liquid bismuth and lead, Journal of the iron and steel institute 3 (1960) 319–323.

[12] G.W. Wilson et al., Study of compatibility of some creep resistant steels with liquid bismuth in non isothermal systems, Journal of the Iron and Steel Institute 190 (1958) 271–276.

[13] G.W. Horsley, J.T. Maskrey, The corrosion of 2.25Cr–1Mo steel by liquid bismuth, Journal of the Iron and Steel Institute 189 (1958) 139–148.

[14] R.E. Deville, W.R. Foley, Liquid metal fuel reactor experiment: liquid bismuth dynamics corrosion tests, HAW-1253, Babcock and Wilcox Company, 1960.

[15] C.H. Waide, L.E. Kukacka, R.A. Meyer, et al., Uranium–bismuth in-Pile corrosion test loop, radiation loop No.1, BNL-736 (T-265), Brookhaven National Laboratory, 1961.

[16] D.W. Dawe, G.W. Parry, G.W. Wilson, Study of compatibility of some creep resistant steels with liquid bismuth in non-isothermal systems, Journal of British Nuclear Energy Conference 5 (1960) 24–29.

[17] H.R. Stephan, W. J. Koshuba, Circulation of bismuth at elevated temperatures, progress report on project 2-01, NEPA-1675, NEPA Division Fairchild Engine and Airplane Corporation, 1950.

[18] R. Cygan, Circulation of lead–bismuth eutectic at intermediate temperatures, North American Aviation Report, NAA-SR-253, 1953.

[19] R. Cygan, Lead–bismuth eutectic at intermediate temperatures, North American Aviation Report, NAA-SR-1060, 1954.

[20] J.C. Clifford, A loop for circulating liquid lead–bismuth mixtures corrosion studies and operation, Ph.D. thesis, Iowa State University of Science and Technology, 1960.

[21] A.J. Romano, C.J. Klumet, D.H. Gurinsky, The investigation of container materials for Bi and Pb alloys, Part I, thermal convection loops, Brookhaven National Laboratory Report, BNL-811, 1963.

[22] G. Ilincev, Research results on the corrosion effects of liquid heavy metals Pb, Bi and Pb–Bi on structural materials with and without corrosion inhibitor, Nuclear Engineering and Design 217 (2002) 167–177.

[23] O.F. Kammerer, Zirconium and Titanium inhibit corrosion and mass transfer of steels by liquid heavy metals, Transactions of the American Institute of Mining and Metallurgical Engineers 212 (1958) 20–25.

[24] J.R. Week, Lead, bismuth, tin and their alloys as nuclear coolants, Nuclear Engineering and Design 15 (1971) 363–372.

[25] H. Glasbrenner, G. Groschel, Exposure of pre-stressed T91 coated with TiN, CrN, and DLC to Pb–55.5Bi, Journal of Nuclear Materials 356 (2006) 213–221.

[26] E.P. Loewen, H.J. Yount, K. Volk, A. Kumar, Layer formation on metal surfaces in lead–bismuth at high temperatures in presence of zirconium, Journal of Nuclear Materials 321 (2003) 269–280.

[27] J.R. Weeks, C.J. Klamut, Reactions between steel surfaces and zirconium in liquid bismuth, Nuclear Science and Engineering 8 (1960) 133–147.

[28] N. Li, Active control of oxygen in molten lead–bismuth eutectic systems to prevent steel corrosion and coolant contamination, Journal of Nuclear Materials 300 (2002) 73–81.

[29] I.V. Gorynin, G.P. Karzov, V.G. Markov, V.S. Lavrukhin, V.A. Yakovlev, Structure materials for power plants with heavy liquid metals as coolants, in: Proceedings: Heavy Liquid Metal Coolants in Nuclear Technology (HLMC-98), vol. 1, Obninsk, Russia, 1998, p. 120.

[30] C. Fazio, G. Benamati, C. Martini, G. Palombarini, Compatibility tests on steels in molten lead and lead–bismuth, Journal of Nuclear Materials 296 (2001) 243–248.

[31] G. Muller, G. Schumacher, F. Zimmermann, Investigation on oxygen controlled liquid lead corrosion of surface treated steels, Journal of Nuclear Materials 278 (2000) 85–95.

[32] G. Benamati, P. Buttol, V. Imbeni, C. Martini, G. Palombarini, Behavior of materials for accelerator driven systems in stagnant molten lead, Journal of Nuclear Materials 279 (2000) 308–316.

[33] O.I. Eliseeva, V.P. Tsisar, V.M. Fedirko, Y.S. Matychak, Changes in the phase composition of an oxide film on EP823 steel in contact with stagnant lead melt, Materials Science 40 (2) (2004) 260–269.

[34] V.P. Tsisar, O.I. Eliseeva, V.M. Fedirko, V.A. Lopushans'syi, Corrosion behavior of α-Fe and 20Kh13 steel in contact with oxygen-containing lead melts, Materials Science 39 (4) (2003) 539–544.

[35] O.I. Eliseeva, V.P. Tsisar, Corrosion of 20Kh13 steel in lead melts saturated with oxygen, Materials science 41 (5) (2005) 603–608.

[36] V.M. Fedirko, O.I. Eliseeva, V.I. Kalyandruk, V.A. Lopushans'kyi, Effects of admixtures of oxygen on the oxidation of iron and Fe–Cr alloys in lead melts, Materials Science 33 (3) (1997) 358–363.

[37] V.M. Fedirko, O.I. Eliseeva, V.I. Kalyandruk, V.A. Lopushans'kyi, Corrosion of Armco iron and model Fe–Cr–Al alloys in oxygen-containing lead melts, Materials Science 33 (2) (1997) 207–211.
[38] H. Glasbrenner, J. Konys, G. Mueller, A. Rusanov, Corrosion investigations of steels in flowing lead at 400 °C and 550 °C, Journal of Nuclear Materials 296 (2001) 237–242.
[39] G. Benamati, C. Fazio, H. Piankova, A. Rusanov, Temperature effect on the corrosion mechanism of austenitic and martensitic steels in lead–bismuth, Journal of Nuclear Materials 301 (2002) 23–27.
[40] F. Gnecco, E. Ricci, C. Bottino, A. Passerone, Corrosion behavior of steels in lead–bismuth at 823 K, Journal of Nuclear Materials 335 (2004) 185–188.
[41] L. Soler, F.J. Martin, F. Hernandez, D. Gomez-Briceno, Corrosion of stainless steels in lead–bismuth eutectic up to 600 °C, Journal of Nuclear Materials 335 (2004) 174–179.
[42] F.J. Martin, L. Soler, F. Hernandez, D. Gomez-Briceno, Oxide layer stability in lead–bismuth at high temperature, Journal of Nuclear Materials 335 (2004) 194–198.
[43] Y. Kurata, M. Futakawa, S. Saito, Comparison of the corrosion behavior of austenitic and ferritic/martensitic steels exposed to static liquid Pb–Bi at 450 and 550 °C, Journal of Nuclear Materials 343 (2005) 333–340.
[44] D. Gomez Briceno, L. Soler Crespo, F.J. Martin Munoz, F. Hernandez Arroyo, Influence of temperature on the oxidation/corrosion process of F82Hmod. Martensitic steel in lead–bismuth, Journal of Nuclear Materials 303 (2002) 137–146.
[45] T. Furukawa, G. Muller, G. Schumacher, A. Weisenburger, A. Heinzel, K. Aoto, Effect of oxygen concentration and temperature on compatibility of ODS steel with liquid, stagnant $Pb_{45}Bi_{55}$, Journal of Nuclear Materials 335 (2004) 189–193.
[46] F. Barbier, G. Benamati, C. Fazio, A. Rusanov, Compatibility tests of steels in flowing liquid lead–bismuth, Journal of Nuclear Materials 295 (2001) 149–156.
[47] J. Zhang, N. Li, Y. Chen, A.E. Rusanov, Corrosion behaviors of US steels in flowing lead–bismuth eutectic (LBE), Journal of Nuclear Materials 336 (2005) 1–10.
[48] G. Muller, A. Heinzel, J. Konys, G. Schumacher, A. Weisenburger, F. Zimmermann, V. Engelko, A. Rusanov, V. Markov, Results of steel corrosion tests in flowing liquid Pb/Bi at 420–600 °C after 2000 hours, Journal of Nuclear Materials 301 (2002) 40–46.
[49] G. Muller, A. Heinzel, J. Konys, G. Schumacher, A. Weisenburger, F. Zimmermann, V. Engelko, A. Rusanov, V. Markov, Behavior of steels in flowing liquid PbBi eutectic alloy at 420–600 °C after 4000–7200 hours, Journal of Nuclear Materials 335 (2004) 163–168.
[50] C. Fazio, I. Ricapito, G. Scaddozzo, G. Benamati, Corrosion behavior of steels and refractory metals and tensile features of steels exposed to flowing PbBi in the LECOR loop, Journal of Nuclear Materials 318 (2003) 325–332.
[51] G. Benamati, A. gessi, P.Z. Zhang, Corrosion experiments in flowing LBE at 450 °C, Journal of Nuclear Materials 356 (2006) 198–202.
[52] F. Balbaud-Ceierier, P. Deloffre, A. Teriain, A. Rusanov, Corrosion of metallic materials in flowing liquid lead–bismuth, Journal of Physics IV France 12 (2002) Pr8-177-Pr8-190.
[53] P. Deloffre, F. Balbaud-Celerier, A. Terlain, Corrosion behavior of aluminized martensitic and austenitic steels in liquid Pb–Bi, Journal of Nuclear materials 335 (2004) 180–184.
[54] G. Ilincev, D. Karnik, M. Paulovic, A. Doubkova, The impact of the composition of structural steels on their corrosion stability in liquid Pb–Bi at 500 and 400 °C with different oxygen concentrations, Journal of Nuclear Materials 335 (2004) 210–216.
[55] M. Kondo, M. Takahashi, T. Suzuki, K. Ishikawa, K. Hata, S. Qiu, H. Sekimoto, Metallurgical study on erosion and corrosion behaviors of steels exposed to liquid lead–bismuth flow, Journal of Nuclear materials 343 (2005) 349–359.
[56] F. Barbier, A. Rusanov, Corrosion behavior of steels in flowing lead–bismuth, Journal of Nuclear Materials 296 (2001) 231–236.
[57] M. Kondo, M. Takahashi, N. Sawada, K. Hata, Corrosion of steels in lead–bismuth flow, Journal of Nuclear Science and Technology 43 (2006) 107–116.
[58] D. Fomez Briceno, F.J. Martin Munoz, L. Soler Crespo, F. Esteban, C. Torres, Behavior of F82H mod. Stainless steel in lead–bismuth and temperature gradient, Journal of Nuclear Materials 296 (2001) 265–272.
[59] C.S. Tedmon Jr, The effect of oxide volatilization on the oxidation kinetics of Cr and Fe–Cr alloys, Journal of the Electrochemical Society 113 (1966) 766–768.
[60] J. Zhang, N. Li, Analysis on liquid metal corrosion–oxidation interaction, Corrosion Science 49 (2007) 4154–4184.
[61] J. Zhang, N. Li, Oxidation mechanism of steels in liquid-lead alloys, Oxidation of Metals 63 (2005) 353–381.
[62] R.G. Ballinger, J. Lim, An overview of corrosion issues for the design and operation of high-temperature lead- and lead–bismuth-cooled reactor systems, Nuclear Technology 147 (2004) 418–435.